NTNU
Norwegian University of
Science and Technology

Localization of a Floating Buoy in a Fish Farming Pen

Håkon Bergerud Grundnes

Master of Science in Cybernetics and Robotics
Submission date: June 2016
Supervisor: Amund Skavhaug, ITK

Norwegian University of Science and Technology
Department of Engineering Cybernetics

Title: Localization of a Floating Buoy in a Fish Farming Pen

Student: Håkon Bergerud Grundnes

Problem description:

The candidate is going to propose a system for localizing a floating buoy inside a fish farming pen. This work includes following sub-tasks.

- Explore relevant concepts of localization
- Investigate sensor solutions
- Choose and test sensors
- Propose a feasible system solution
- Evaluate suitability of system

Responsible professor: Amund Skavhaug, ITK

Abstract

This thesis proposes a solution to localize a floating buoy in a fish farming pen. The task is provided by Stingray Marine Solutions and is meant to be an integrated part of their optical delousing system. The solution proposed uses ultra-wideband ranging sensors (DecaWave DW1000) to measure the distance from three anchor nodes to a tag on the buoy. The sensors were tested using a test kit delivered by DecaWave. To validate the sensors' suitability for the localization task, several test cases were designed. The test cases were designed to test the sensors localization abilities and robustness in an environment similar to the expected environment in a fish farming pen. Two different setup configurations of the anchor nodes were examined. One with the anchor nodes positioned on a line and one were the anchors were distributed around the edge of the pen. Through simulations and experimental tests, it was concluded that the best setup of the nodes was to be distributed around the pen edge. By using a Kalman filter or a Least squares estimator, the system achieved to localize a stationary tag within a distance of 10 and 14 centimeters respectively for 96% of the sample points.

The tests examining the feasibility of using the sensors in a relevant environment showed that the sensors were able to perform sufficiently when the antenna was slightly above the water surface. When lowered such that there was significant amount of water between the anchor antennas and the tag the signal was lost.

Because of the promising results in this thesis, it was proposed to go through with developing appropriate sensor modules and testing said modules in a fish farm pen.

Sammendrag

Denne oppgaven foreslår en løsning for å lokalisere en flytende bøye i en fiskemerd. Oppgaven er skrevet for Stingray Marine Solutions og er ment å integreres inn i deres system for optisk avlusing. Løsningen foreslått bruker ultra-wideband radio sendere (DecaWave DW1000) for å måle avstand fra tre ankernoder til en målnode på bøyen. Sensorene ble testet ved bruk av en testpakke som DecaWave tilbyr. For å validere sensorenes egnethet til bruk i denne oppgaven ble flere testscenarioer satt opp. Testscenarioene ble utformet for å teste sensorenes lokaliseringsevne og hardførhet i et miljø tilsvarende det forventede miljøet i en fiskemerd. To forskjellige oppsett av sensorene ble undersøkt. En hvor ankernodene var plassert på en flat linje og en annen hvor ankernodene omslutted fiskemerden. Gjennom simulering og praktiske forsøk ble det konkludert at det var best å plassere sensorene slik at de omsluttet fiskemerden. Ved å bruke et Kalmanfilter ble en stasjonær målnode lokalisert med en feil på under 10 centimeter for 96% av målingene. For en minstekvadratsestimator ble en feil på 14 centimeter oppnådd i samme test.

Testene som undersøkte nøyaktigheten og egnetheten til sensorene i et aktuelt miljø viste at sensorene var i stand til å funksjonere i tilstrekkelig grad så lenge antennen var så vidt over vannoverflaten. Når målnoden ble senket slik at det var en betydelig mengde vann mellom antennene til mål og ankernoder ble signalet mellom radiosenderene tapt.

På grunn av de lovende resultatene i denne oppgaven er det anbefalt å gå videre med design av passende sensor moduler og testing av disse i fiskermerder.

Preface

This thesis is submitted in partial fulfillment of the requirements for the Master of Science degree at the Norwegian University of Science and Technology.

Being given the opportunity to work on an industrial problem has been inspiring and I have gained a lot of knowledge and experience in the five months that I have worked on this problem. The sea lice problem is substantial and being able to give a small contribution to a greater cause has been rewarding.

First, I would like to thank my supervisor Amund Skavhaug and my fellow students at NTNU for five great years. Good fortunes and gratitudes are also directed at the three people who helped me conducting the field tests, Knut Brekke, Nicolay Erlbeck and Oliver Grundnes. Lastly, I would like to thank Stingray Marine Solutions for giving me the project.

Contents

List of Figures

List of Tables

Glossary

Absolute Bandwidth	Difference between upper and lower of -10 dB emission point.
anchor	A anchor is a reference node used to estimate the position of an object (Tag) by knowing the distance from several anchors to the object and the anchors' positions.
Buoy Unit	Buoy unit (BU) is the floating buoy part of the delousing system and is the object to be localized in this thesis.
center anchor	Anchor placed inside or adjacent to the locker next to the fish pen.
Extended Kalman Filter	The Extended Kalman Filter (EKF) is a way of applying the Kalman Filter to non-linear systems.
Least Square Estimator	The Least Square Estimator (LSE) estimates states by minimizing the sum of squared errors between the measurements and corresponding measurement functions.
Polyoxymethylene	Thermo plastic material used in construction of the BU and submerged unit (SU).
remote anchor	Anchors located outside of the locker next to the fish pen.

tag	The node to be localized.
Time of Flight	Time of Flight (TOF) is a measurement technique where the travel time of a signal is used to estimate a distance.
Trilateration	Determining position from a set of range measurements..

Acronyms

AOA Angle of Arrival.

BU Buoy Unit.

CDF Cumulative Distribution Function.

DOF degrees of freedom.

DOP Dilution of Precision.

EKF Extended Kalman Filter.

GNSS Global Navigation Satellite System.

GPS Global Positioning System.

IC integrated circuit.

IMU inertial measurement unit.

IR impulse radio.

KF Kalman filter.

LOS line-of-sight.

LS least square.

LSE Least Square Estimator.

MC microcontroller.

ML maximum likelihood.

MPC multipath component.

NLOS non-line-of-sight.

NTNU Norwegian University of Science and Technology.

NTNUI Norwegian University of Science and Technology's Sports Association.

POM Polyoxymethylene.

RF radio frequency.

RMS root mean square.

RMSE Root Mean Square Error.

RSS Received Signal Strength.

RTLS Real-time Locating System.

SMS Stingray Marine Solutions.

SPI serial peripheral interface.

SU submerged unit.

TDOA Time Difference of Arrival.

TOA Time of Arrival.

TOF Time of Flight.

TWR two way ranging.

TWTOF Two-way Time of Flight.

USB Universal Series Bus.

UWB ultra-wideband.

Chapter 1
Introduction

Seafood is the second largest export in Norway only surpassed by oil & gas. The seafood harvest can be divided into two different sections, fish from capture and fish from aquaculture. With a growing global population, the world needs an effective way of producing protein and fish from aquaculture has a high potential of supplying this demand. Compared to other popular protein sources such as cattle, pork or chicken, fish farming has big advantages considering its environmental footprint. A commonly used indicator of the environmental advantages of fish farming versus land based protein is how well the animals convert their food into body mass. Where it takes at least 4 kilograms of food to produce 1 kilogram of cattle, Marine Harvest claims they only need 1.12 kilograms to produce 1 kilogram salmon[3, p.7]. Other numbers[2, p.16] show that the feed conversion rate is slightly higher when taking entire pens into account. This is because the numbers include lost or dead salmons as well. It is believed that the increase in the amount of dead salmon is connected to the sea lice problem and largely due to handling of salmon during delousing. Chicken and pork does not need as much food as cattle to produce one kilo of body mass, but they are still inferior to salmon with respect to their conversion of food. With salmon having a higher percentage of body weight being edible meat as well, salmon farming is one of the most resource efficient methods of protein production. Conveniently, salmon is by far the most common aquaculture fish with more than 2500 fish pens across Norway.

1.1 The sea lice problem

Sea lice are small marine parasites sitting on the outside of the fish feeding on the fish's mucus, tissue and blood. To survive its host's immune defense, the sea lice release immunosuppressive saliva. Together with the open wounds the lice inflict on the host, the saliva makes the fish more exposed to infections. In addition, a large enough number of sea lice can make the salmon stressed and reduce the salmon's appetite, causing a lower biomass output for the salmon farmers. There is also a

Figure 1.1: A salmon being optically deloused. The laser fills the louse with energy which causes it to coagulate. Courtesy of Stingray Marine Solutions.

growing concern regarding sea lice spreading to the wild salmon population.

As the sea lice is a heavy burden on the salmon industry, a great number of measures have been taken to cope with the sea lice problem. Some examples of techniques used to remove lice are medicine/chemicals, cleaner fish, warm water or lice nets. Sea lice removal is considered the highest one cost component in salmon farming disregarding the cost of feed and nutrition.

1.2 Stingray Marine Solutions

Even though there is a substantial number of methods to fight sea lice, most of them require man power or handling of the fish in some way. Additionally, some of them comes with environmental effects such as toxicity or high energy use. Many of the treatments are done in a reactive manner. Removing the lice after they have become a substantial problem often leads to large scale operations that are expensive. These are disadvantages Stingray Marine Solutions (SMS) try to avoid when offering a product that is continuously removing sea lice. Stingray's patented *optical delousing* is a method using computer vision to identify and track sea lice attached to the salmon's body and focused laser beams to remove them. A submerged unit (SU) containing a computer, camera and laser is connected to a floating Buoy Unit (BU) and submerged into the fish pen where it can work for twenty-four hours a day. When the salmons swim by the camera the computer makes a decision and fires the laser if a louse is detected. The laser fills the sea lice with energy and causes

them to coagulate. Because of the shells covering the salmon's body, the laser will be reflected off the salmon and do it no harm.

1.3 Localization Problem

To be able to deliver the best service possible, it is desired from SMS' part to have accurate information about the position of the BU and SU. Possessing this information is considered valuable as it will offer a new range of features for SMS to add to their current system. Accurate localization data can be incorporated into a graphical user application, tagged in logging data and used to control the position of the BU. There are even possibilities that the position data can be used to find patterns in the fish distribution across the fish pen. Such information could prove to be extremely valuable for research purposes or to optimize the laser unit's position throughout the day. The application areas just described are just a few of the possible applications accurate localization data offers.

1.3.1 Earlier attempts

An external company was involved during an earlier phase of solving the localization problem. They offered a solution using a Global Positioning System (GPS). However, after some testing, the solution was deemed unsatisfying as there were severe problems with receiving signals from the GPS satellites. The reasons for the signal problems remain unclear, but it is assumed that the problems might be due to the multipath components (MPCs) reflected of the water surface. Other potential explanations might be the disturbances of the surroundings (electronics surrounding the GPS device) or shielding caused by the covers needed to protect the GPS.

Due to the insufficient results with the GPS solution, another alternative strategy were desired. The idea of using a GPS were not fully discarded yet, but it was considered more likely to be a success as part of a hybrid solution. The GPS could acquire a global position estimation of a point less exposed to noise and then use some other solution to get the position of the BU relative to the GPS.

Format of Thesis

The scope of this thesis has been to investigate the feasibility of a hybrid solution where it is assumed that the position of the fish pen is already known. This includes looking into feasible sensor techniques, ways of using sensor data to localize the buoy, find suitable sensors, test sensors and look into ways to filter the data. Due to time restrictions, the scope does not include making a prototype of a solution and integrate it onto the current system.

The thesis will be used by the employees at SMS who will evaluate whether or not to continue with the solution described. The background of the employees at SMS varies from computer scientists to mechanical engineers, but there are few people with a cybernetics background. Because of this, the thesis includes descriptions of some concepts that might be basic to people familiar with the subjects, but are necessary to understand and implement the solution.

The second chapter describes and discusses different sensor alternatives while chapter 3 describes possible ways of constructing and setting up the system. Then follows a chapter presenting and discussing the relevant state estimation techniques and considerations affecting their localization accuracy. In chapter 5, several test cases for examining and validating the feasibility of the solution are presented. Chapter 6 decribes the system models used. Some of the cases were simulated and a description and results of said simulations are found in chapter 7. The practical testing and results of the sensor cases are presented in chapter 8 and followed by a summarizing discussion in chapter 9. The overall conclusion is found in chapter 10.

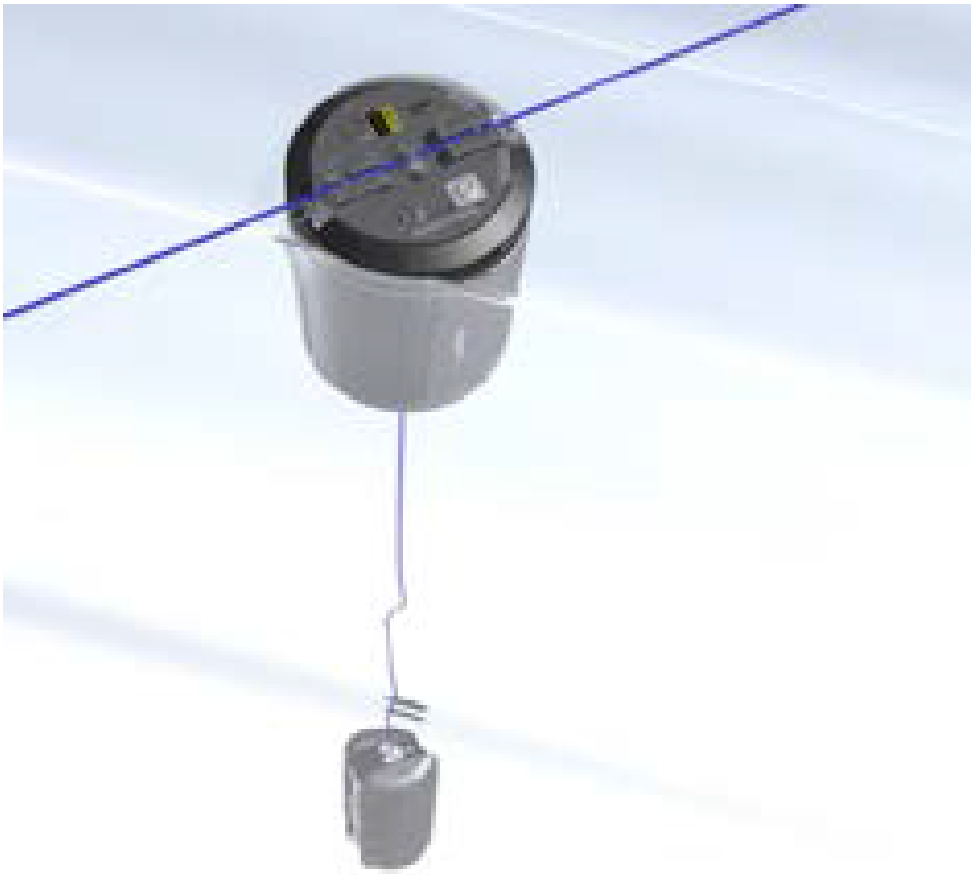

Figure 1.2: A floating Buoy Unit (BU) connected to a wire stretched across the fish pen and a submerged unit (SU) connected to the BU. Courtesy of Stingray Marine Solutions.

Chapter 2
Sensoring and measurement techniques

There are many feasible options when choosing sensors to localize the BU, ranging from optical sensors to radio frequency (RF) sensors or odometry sensors like inertial measurement units (IMUs). This chapter describes feasible sensor solutions and discusses their suitability for this project. The chapter will also justify the decisions made in the project regarding the choice of sensors.

2.1 Global Positioning System

There is one commercial product that immediately stands out when thinking about outdoor localization, GPS. They are the most known type of Global Navigation Satellite System (GNSS) and can be found in cars, smart-phones and various navigation products. Even though the main output is usually an absolute position, they can be used to get the orientation as well[16].

The following short description of GPS is mostly from [19, p.21-25] The principles of GPS/GNSS are as follows. Numerous GPS satellites orbits the earth with a known position at any given time. The satellite transmits radio signals with a time-stamp. The transit time of the signal from satellite k is then measured by the ground device. The GPS satellites carry atomic clocks that are synchronized to such a degree that no drift is assumed. The receiving device records the time the signal is received and compares it to the time stamp in the transmitted signal. The transit time along with the constant speed of light that the radio signal propagates with is then used to calculate the measured range between the ground device and satellite k. The relation between the measured distance, the positions of the ground device and a given satellite (k) is described in equation 2.1.

$$\rho^k = \sqrt{(x^k - x)^2 + (y^k - y)^2 + (z^k - z)^2} - b \tag{2.1}$$

Where x^k, y^k, z^k and ρ^k are the x-y-z-coordinates of the satellite along with the measured distance to the ground device. x, y and z are the coordinates of the ground device. The b in the equation above is added to compensate for the clock bias on the ground device. Because the GPS receivers usually lacks an atomic clock, a bias often occur when measuring the transit time. To compensate the clock drift on the ground device, a constant bias b is added to the equation. This bias will be the same for all range measurements as the satellite clocks are almost perfectly synchronized. The position of the satellite can be estimated to the accuracy of a few meters based on predictions made up to 48 hours earlier. This leaves four unknowns (x, y, z and b), hence measurements from four satellites are needed. More satellites than four can be used to improve the accuracy.

2.2 Optical Sensors

Another possible solution would be using a camera (computer vision), laser ranging or other optical sensors. Laser rangers and cameras are often used with autonomous robots[21] where they are typically mounted on the robot[23] and perceiving the world around[12]. Camera sensors do not necessarily have to be placed on the BU as there are examples where they are used in a network surrounding the tag[14]. However, optical sensors have a disadvantage in that they need a clear visual contact with the BU. As the fish pens are located at sea a likely scenario would be that during the winter months the lenses could be covered with snow or dirt which would inhibit the system from localizing the BU. The likelihood of this scenario could probably be reduced by adding some form of screen to protect the lenses, however, sometimes bad weather such as fog might cause visual problems that screening would not prevent. As the natural light differs a lot throughout the day, issues regarding light might create difficulties as well.

2.3 Inertial measurements units

Another possibility is using an IMU inside the BU. IMUs use three orthogonal accelerometers and gyroscopes. These measure acceleration along and angular velocity about three orthogonal axes aligned to its own inertial frame. When the acceleration is known, it can be integrated one and two times to get velocity and position respectively. In the same manner the angular velocity can be integrated to get the orientation. Additionally, some IMUs include a compass or magnetometer as well. Because the orientation is known, it will be possible to calculate the acceleration along the global axes. This acceleration can also be integrated to estimate the velocity and position of the IMU. However, IMUs often suffer from drift as a result of small measurement errors being summed up through integration[15]. The single and double integration to get speed and velocity lead to a linear and quadratic errors respectively.

Because of this, IMUs are often used together with other sensors that are able to compensate the drifting error[18].

2.4 Radio Frequency Localization

The GPS described in section 2.1 is probably one of the most commonly known applications for radio frequency (RF) localization. It gives the global coordinates and for reasons discussed in section 2.5 was not chosen to localize the BU. Still, the project uses similar techniques such as trilateration, Time of Flight (TOF) and RF signals.

2.4.1 Ultra-wideband

Ultra-wideband (UWB) devices have become quite common to use when localizing objects. They are particularly popular indoors [20] because of their robustness against MPCs and ability to penetrate obstacles.

The information in the following section is extracted from [10, chapter 2, p. 20-42]. A radio signal is typically called a UWB signal if one of two conditions hold. The Absolute Bandwidth (Equation 2.2) is at least 500 MHz or the fractional bandwidth (Equation 2.3) is bigger than 0.2. Absolute bandwidth is defined as the difference between the higher and lower frequencies (f_H and f_L) of the -10 dB emission points.

$$B = f_H - f_L \tag{2.2}$$

The fractional bandwidth is the absolute bandwidth divided by the center frequency (f_c) of the frequency band.

$$B_{frac} = \frac{B}{f_c} \tag{2.3}$$

As opposed to other RF-ranging techniques, UWB solutions do not necessarily use a carrier wave as reference when sending information. Instead, it sends short pulses that contains a wider band of frequencies. The signal is modulated by defining time windows containing a number of slots (e.g four). By varying which time slot the pulses are being sent, one can alter the information that the signal contains. Such a configuration is called impulse radio (IR).

Using a wide frequency band allows the signal to be sent with lower power on each frequency making it useful for applications needing low power consumption. Another huge advantage with this is its robustness when it comes to noise. Covering

a large frequency spectrum makes the signal more resilient to noise components at certain frequencies. In [10], the main advantages of using UWB for localization applications is summarized in the following way.

- penetration through obstacles
- high ranging, hence positioning accuracy
- high-speed data communications
- low cost and low power implementation.

As seen from the list above, using UWB as a ranging technique has many advantages. Another advantage using pulse based radio signals is that there is no need for the receiving node to lock onto the transmitted signal. With GPS, the receiver needs to lock into the pseudo random signal it receives and search through the signal to get the correct time stamp. With UWB, there is no need for routines that require searching as it only deals with pulses. In an uncertain environment where waves might cover the BU at times, this could prove to be a huge advantage.

Gaussian waveform

There are several waveforms that can be used to generate a signal with UWB properties. Some examples are Hermite polynomials, wavelet pulses and the Gaussian pulse. The Gaussian pulse can be expressed as

$$\omega(t) = \frac{A}{\sigma\sqrt{2\pi}} e^{-\frac{t^2}{2\sigma^2}} \tag{2.4}$$

By changing A and σ the energy and width of the signal can be altered respectively. An example of the Gaussian waveform and its derivatives can be seen in Figure 2.1.

Figure 2.2 shows the frequency plot of the Gaussian waveform and different orders of its derivative. Changing the signal waveform gives control over the frequency spectrum the signal contains.

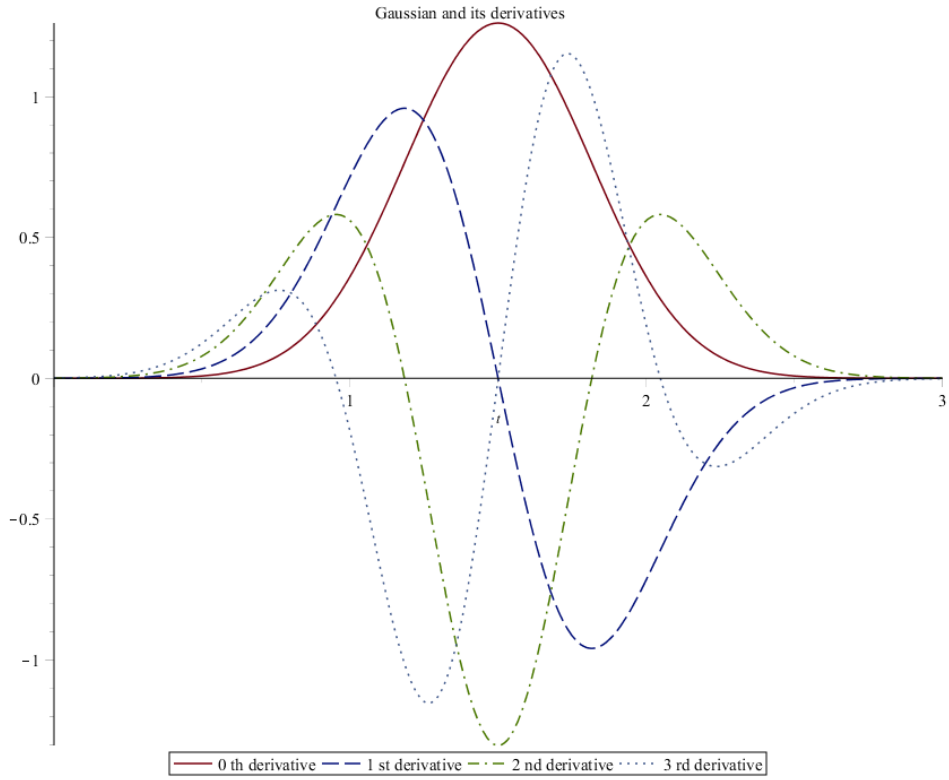

Figure 2.1: The Gaussian waveform and its derivatives are examples of signals used when transmitting UWB signals. The signals have the property of containing many more frequencies than a single sine wave. This property is useful when considering the signal's robustness. Figure generated using Maple 2015.

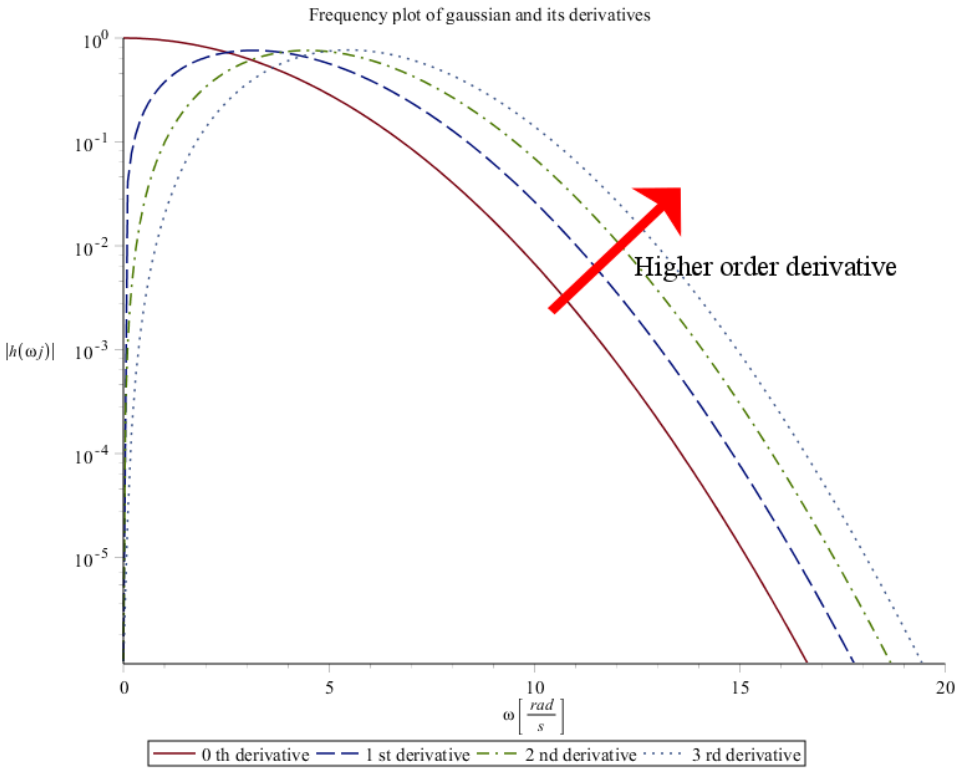

Figure 2.2: Frequency plot of the Gaussian waveform and its derivatives. As seen from the figure, different orders of the derivative contains different frequency spectrum. Figure generated using Maple 2015.

2.4.2 RF localization techniques

Because of the properties of RF signals, there are numerous ways they can be used to get positional data. Many of the techniques are based on the properties of RF signals when propagating through air, that is, the speed the signal travels with is approximately constant. This means that many of the localization techniques used to get positional data measures the travel or arrival time of the signal in some way. Another property that can be used is the strength of the signal.

Received signal strength (RSS)

As the power of the received signal can be measured and there are models describing the relation between distance and power loss, it is possible to use the Received Signal Strength (RSS) to estimate the distance between two nodes. This also assumes the

transmit power is known. Unfortunately, RSS estimators are considered to be less accurate than other RF approaches that are time based[10, p. 101].

Time of Arrival (TOA)

The Time of Arrival (TOA) approach takes advantage of the constant speed of radio waves through air. The approach assumes the transmitting time of the signal is known and measures the time when the signal is received at each node. When this is known the travel time can be calculated and the distance can be calculated as seen in Equation 2.5.

$$d_{TOA} = (t_T - t_R) * c \tag{2.5}$$

Where t_T is the transmit time, t_r is the receive time and c is the speed of light. A challenge with using this approach is the synchronization of the clocks at each node. If the clocks of the two nodes are not common, time information must be shared through some relevant protocol.

Time Difference of Arrival (TDOA)

Another possible technique is the Time Difference of Arrival (TDOA) approach. The tag node transmits a signal and a number of reference nodes receive it. As opposed to TOA, there is no need to sync the clock on the tag node with the clocks on the reference nodes, but the clocks on the reference nodes need to be synchronized. The measurements in the TDOA estimators are the differences of the received time on the reference nodes. These measurements define hyperbolas where the tag node can be located. Problems using the TDOA estimator are that it requires an extra reference node and the reference clocks need to be synchronized.

Angle of Arrival

Unlike the other approaches described earlier that provide range information, the Angle of Arrival (AOA) measurement provides information about the angle it receives the signal. It does so by having several antenna elements in an array and measure the time difference of the signal's arrival at each element. Using a setup with an AOA measurement could be favorable if it is combined with a range measurement as only one external node outside the BU would be needed. This is because knowing the angle and distance would make the x-y coordinates available through polar coordinates. A problem with AOA measurements is that the precision of the localization becomes significantly poorer when the signal arrives at a steeper angle. This means that using an AOA sensor might leave zones at the edges of the pen with too low precision. A way to make up for this could be to make the sensor follow the movement of the tag to keep the tag orthogonal to the antenna array, but such an approach is discarded for this project as other techniques are rather used.

Two-way Time of Flight

Another way of localizing the tag is having the tag send a message to each reference node, then wait for an answer and measure the round trip time. An advantage using this approach is that there is no need to synchronize the clocks on the different nodes as the round trip time is only measured at the tag. However, there will be a delay when the reference node is processing the signal and it's important this delay is measured. Information about the processing time on the reference node needs to be delivered to the tag, but this could be done through some radio protocol. The calculation of the distance for the Two-way Time of Flight (TWTOF) scheme can be seen in Equation 2.6.

$$d_{TWTOF} = \frac{t_R - t_T - t_P}{2} * c \tag{2.6}$$

Where t_R is the receive time at the tag node, t_T is the time at which the tag transmits the signal, t_P is the processing time on the reference node and c is the speed of light. The round-trip time includes both directions and needs to be divided by 2.

2.5 Sensor choice

Considering the different sensor alternatives described earlier, numerous solution alternatives present themselves. The simplest one would probably be to mount a GPS on the BU that will provide the global coordinates. As the GPS could have provided x-y-z coordinates, the localization problem of the BU would have basically been solved. During earlier phases of the project SMS outsourced the localization task to an external company. This company proposed a solution using a Piksi GPS [6] to get the position of the BU. The GPS had severe problems receiving a signal and is considered unsuited to be used within the BU. The reasons for the bad performance of the Piksi GPS are still not concluded on. Some possible reasons are noise from the computer systems, shielding from the BU or misconfiguration. Because of these difficulties an alternative solution is desired from SMS's part.

Figure 2.3: The Piksi GPS module was tested in an earlier phase of the project, but due to unsatisfying results an alternative approach is desired. Piksi™- Courtesy of Swift Navigation, Inc. | www.swiftnav.com

As opposed to the GPS that estimates the global coordinates, the other sensors described above require a more local approach. That is, as they cannot measure their position relative to a satellite, their reference will be somewhere on the fish pen. It is believed to be more plausible to make the GPS work outside the BU (e.g in the locker next to the pen). This means that a way of determining the relative position of the BU compared to the GPS is needed. Using such a hybrid approach makes a whole other range of options available.

Laser rangers offer quite good accuracy and are found in many commercial varieties. However, these products often require aiming which might prove to be challenging. Additionally, there is a wish at SMS not to use optical sensors as bad weather conditions and problems regarding sight might occur. SMS focuses a lot on having as little down time as possible and having a localization system that might be hindered by bad weather is not compatible with this ambition.

A challenge using an IMU is the need to know the initial position. The IMU only measures the odometry and the position estimate will only be relative to the starting position. This means that the accuracy of the estimate will only be as good as the initial position estimate. A precise initial estimate is possible to achieve, but the drift of the IMUs will also be a source of error. As the IMUs do not measure their position relative to some other object, they lack a way to compensate for this drift. However, using an IMU in combination with some other sensor setup could be useful as it gives more data and information to take into account.

As described in subsection 2.4.1, UWB sensors have a big potential when it comes to ranging and therefore also localization. This is why it was the sensor technique chosen to be used in this project.

2.6 DecaWave DW1000

Designing RF circuits is a whole separate field of its own and would have been extensive enough for its own master thesis. Luckily, there were alternatives. Trying an already designed RF circuit spared a lot of effort and was expected to perform better than something made in this master thesis.

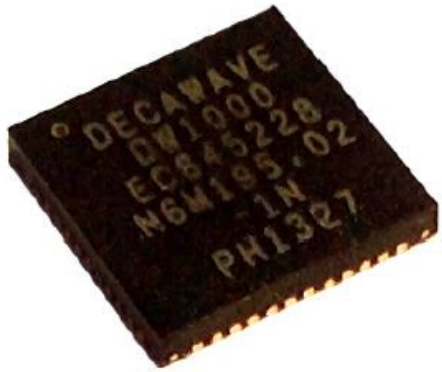

Figure 2.4: The DW1000 integrated circuits (ICs) use UWB radio signals to measure distance between each other. This make them a suitable sensor choice to localize the BU. Courtesy of DecaWawe©| www.decawave.com

The DW1000 IC is a chip developed by the Irish company DecaWave. It uses UWB radio signals for communication and range measuring. Their product brief[8] promises a localization precision of 10 cm and a range up to 300 meters. This should be well within the accuracy desired in the solution. A list of the sensor's attributes can be seen below.

- Long range (up to 300 m)
- High accuracy (within 10 cm)
- Low power consumption
- Supports 6 frequency bands between 3.5 and 6.5 GHz
- Easy integration with many different microcontrollers (MCs) through serial peripheral interface (SPI) interface

- Support for two way ranging (TWR) and TDOA methods
- Hardware and Software test modules are available from DecaWave
- Unit price of around 10 USD.

As the biggest fish pens in Norway have a diameter of approximately 60 meters, a 300 meter range should be sufficient. With a low power consumption, there is a feasibility of using batteries as power source. This is discussed further in subsection 3.3.2. The ability to choose between different frequency bands offers a versatility that can prove to be beneficial as some bands might perform better than others on the given location due to sources of noise that might emerge. The DW1000 IC is controlled through an SPI interface. This means it must be used with another MC where the IC works as a slave taking instructions from the MC through SPI. Another substantial benefit is that there are available test kits, modules and applications from DecaWave. Having the option to try test kits is great as it gives a way of determining if the chip's performance is satisfying without having to design a customized circuit board. This saves a lot of time and gives a quick way confirming/discarding the option of using the DW1000 IC.

Chapter 3
System Construction

Following chapter describes and discusses the different feasible options regarding the construction of the system. This includes an overview of available resources, sensor arrangement and considerations regarding these that need to be taken when applying the localization system. The chapter also defines certain standards that were used throughout the thesis.

3.1 Available components

Locker next to pen

There is a reserved locker next to the pen that Stingray Marine Solutions (SMS) use as part of their operation. The locker, which contains various equipment such as communication devices, is placed at the edge of the pen approximately 2 meter above the water surface. Because of the electronic equipment it contains, a power supply will be available from the locker. This outfit, from this point referenced to as *the locker*, is intended to possess the GPS.

Buoy unit

The Buoy Unit (BU) is the object that is to be localized. It is a floating construction made of Polyoxymethylene (POM), and contains various computers and sensors. A submerged unit (SU), who is doing the delousing, is connected to the BU. The BU floats with only a few centimeter of its lid above the water surface and is connected to a wire that is stretched across the fish pen.

3.1.1 Two different types of pens

Generally, two different types of fish farming pens are being used in the industry today. The most commonly used type is the round fish pen (Figure 3.1a). The round fish pen is usually made of flexible material to make it robust. The pen's flexibility might bring some challenges regarding the positioning of the sensors. If the pen is

(a) Example of round fish pens. The round fish pens are the most common ones and are usually made of flexible material to make them more robust against a rough sea environment. To the bottom right, the locker described in section 3.1 can be seen.

(b) The rigid square fish pens are not as common as the flexible round fish pens.

Figure 3.1: Two different types of fish pens. Courtesy of Stingray Marine Solutions.

squeezed due to external forces like wind, current or waves, the pen will become disfigured and on an elliptic shape. As a result, the position of the remote anchors will be distorted compared to their original position. A consequence of this will be an inaccuracy in the position estimate of the BU. This is a clear disadvantage by using trilateration to find the BU position. Workarounds for this problem is discussed

further in subsection 3.3.2.

The other type of fish pen used is the square fish pen (Figure 3.1b). The square pens are usually rigid which means they do not become disfigured when the weather conditions are rough. This means that the considerations that need to be taken with a circular pen regarding its flexibility are unnecessary with a square pen. However, as having a restriction to the type of fish pen where the application could be used is not an option, the application must be designed to work in both cases.

3.2 Coordinate frame

The application described in this thesis will only find the relative coordinates of the BU. This means that a local coordinate frame that can work as a reference is needed. As mentioned previously, there is a locker available next to each operational pen. Picking a point in the locker to be the origin of the coordinate frame is convenient as it is intended for a GPS to be positioned near the locker. A small distance between the GPS and origin of the local coordinate frame makes it easier to know their exact relation and thus transform from one coordinate frame to another.

The orientation of the coordinate frame is not particularly important as long as all parts of the system using the coordinate frame is coherent to the standard set. For this project different orientations were chosen for different sensor arrangements as it made the various mathematical expressions simpler. An example of a coordinate frame can be seen in Figure 3.2.

Sometimes when doing ranging over long distances, it is necessary to take the earths curvature into account, but as the ranges in this application are relatively small the curvature of the earth is ignored. From now on when mentioning the position of some object, it is the relative position in the local coordinate frame that is referenced and not a global position coordinate.

3.3 Physical setup

The TWTOF approach the DW1000 uses needs reference nodes to be able to localize an object that need to be arranged in a suitable manner. These reference nodes will from now on be known as the anchors. It is necessary to know the position of the anchors in order to locate the BU. As the locker have access to power supply and is chosen to be in proximity of the origin of the local frame, one of the anchor should be placed near or on top of the locker. From now on this node will be referenced as the center anchor or anchor 0.

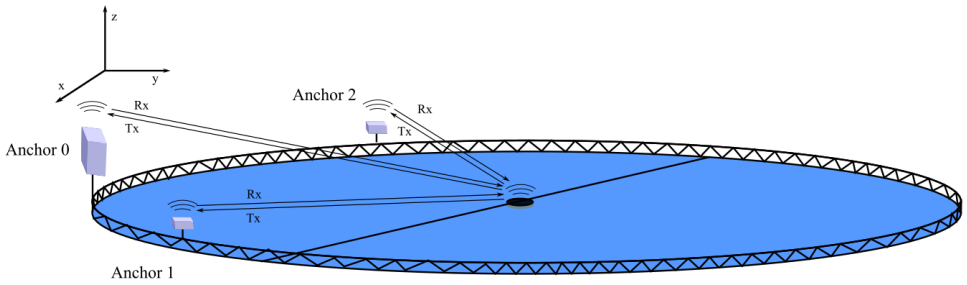

Figure 3.2: The Figure shows the system when using TWTOF. The BU transmits a message to the anchor nodes, waits for the answer and measures the round trip time. Knowing the round trip time makes it possible to calculate the distance. An example of a local coordinate frame can be seen in the top left corner.

To be able to use trilateration and locate the BU, a minimum of two anchors are needed. When only two anchors are used, two solutions will exist. This leads to the system requiring at least three anchors to get a single solution. However, as the test kit used for the field tests only contained three anchors, a setup using three anchors is discussed from this point on. The two remaining sensors have to be placed somewhere around the fish pen and there are different aspects to consider when doing this as their position affects other operations and the performance of the localization. These two remaining sensors will from now on be known as the *remote anchors* as they are not positioned in the origin of the local coordinate frame.

3.3.1 Interference with other operations

As the localization solution this thesis proposes will be used in an industrial environment, the possible interference the setup have with the operations on the fish farm have to be taken into account. The BU localization will be a small feature of the product SMS offer, which is again a sub operation of the total operation on the fish farm. Minimizing the sensor arrangement's interference with the other operations on the fish farm is considered favorable. The placement of the center anchor on top of the locker is in concurrence with this ambition. This leaves the remaining two anchors (remote anchors) to be positioned somewhere else along the edge. However, interfering with other operations is not the only pressing matter and considerations regarding power supply and localization performance must be taken as well.

3.3.2 Power supply of sensor nodes

With the locker having access to power supply and the center anchor being positioned in proximity of the locker, delivering power supply to that node is considered

uncomplicated. The same goes for the tag node within the BU. Regarding the power supply for the remote anchors, two options are considered. The first option is to connect the remote anchors to the power supply in the locker using a wire. This means the wire has to be stretched out along the side of the pen. As there are other operations going on in the fish pen besides delousing, mounting the remote anchors close to the locker is considered favorable as it will reduce the application's footprint on the fish pen. There might be human workers around the fish pen or parts of the fence have to be removed. If the wire would need to be removed or broken, it would be a undesired load on the workers on the fish farm. The localization system requiring a long wire stretched around long parts of the pen edge reduces its compatibility with other ongoing operations on the farm and makes it likelier to be an obstacle.

The second option is to use batteries to power the remote anchors. With no wires needed, the remote anchors' interference with the other operations will be considerably reduced. If the system's life time on one battery pack is of acceptable length, such that the manual changing of batteries is not considered an inconvenience, using batteries is a feasible option. The DW1000 IC has a very low power consumption. OpenRTLS is a collaborative project between different companies specialized in Real-time Locating Systems (RTLSs) that uses the DW1000 chip in their products. They state on their website that their circuit boards, that contains the DW1000 chip, a MC and various other electronic components, can last for five years on a 600mAh battery with a slow duty cycle[7]. A battery life time of one year will probably be sufficient and can likely be increased by increasing the size of the battery pack. It is preferred not to use OpenRTLS' products as their products are relatively expensive and one could make similar boards with similar properties. Making own dedicated circuit boards for the specific task in this application has the advantage, besides the reduced unit price, of leaving out redundant circuitry to get even better battery performance.

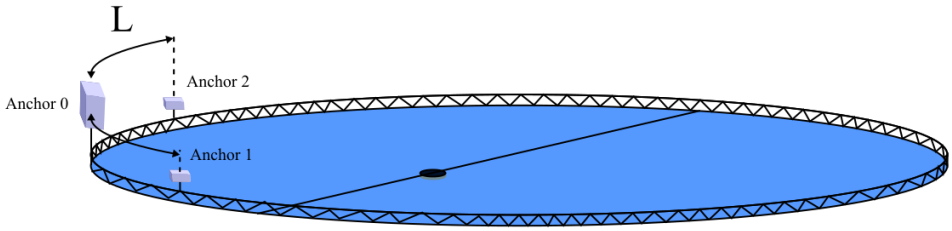

Figure 3.3: Round fish pen with short distance between the anchors for easy wired power supply and a denser setup.

Using wires as power supply instead of batteries reduces the need of optimizing the power consumption of the sensors. This could prove to be advantageous as it

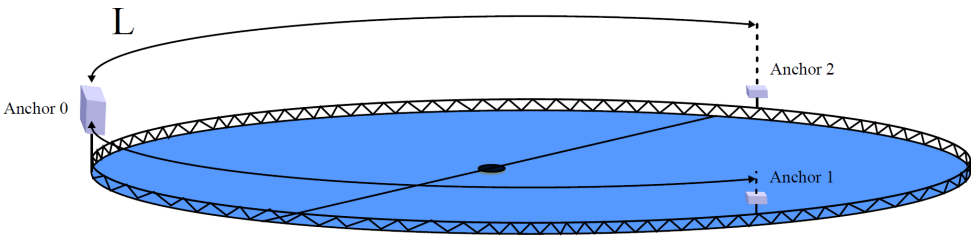

Figure 3.4: Round fish pen with longer distance between the anchors.

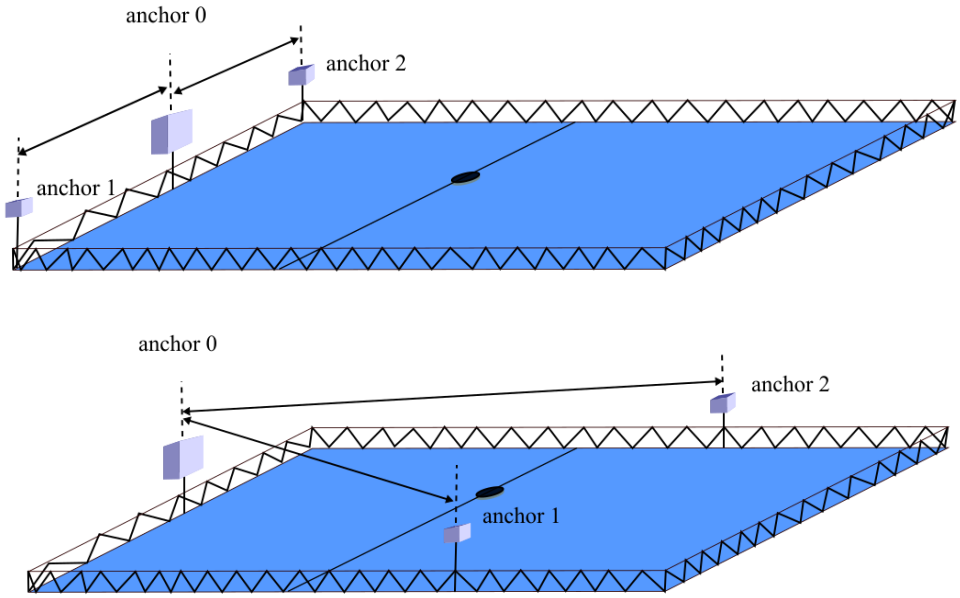

Figure 3.5: Possible setups up for a square fish pen. Similar to the setups in the round pen case(Figure 3.3 and 3.4).

gives the possibility of having a higher update rate of the measurements without having to consider the increased power consumption. A problem with keeping the anchor nodes too narrow is the effect it might have on the localization performance. This is investigated further in section 3.4.

3.3.3 Considerations regarding the disfiguring of the fish pens

As mentioned in subsection 3.1.1, it is possible for the round pens to become disfigured in the case of bad weather. This will lead to errors in the position estimate of the BU as the position of the remote anchors will be different to the initial setup. The

error coming from the disfiguring of the fish pen will be a biased error where the BU position and its estimate will have an offset because of the wrong anchor positions. On the contrary, narrowing the distance between the sensors leads to a larger variance in the position estimate (explored further in subsection 3.4.2). This means a trade-off between the bias and variance of the position estimate have to be considered.

A possible solution to overcome the problems with the disfiguring of the pen is to correct the position of the remote anchors. Placing a GPS on each remote anchor node and use its positional data to update the anchor position is one feasible feasible option. This assumes that the anchors' position above water is high enough. Another way of reducing this effect could be to put the sensors so close to each other that the disfiguring of the fish pen will not affect the sensors' relative position to one another significantly. However, positioning the anchors close reduces the geometric properties of the localization and leads to a worse expected performance (see subsection 3.4.2). Some of the tests described later in this thesis examines the latter option and how well the system could be expected to perform with inconvenient geometric system properties.

3.4 The sensor arrangement's influence on localization performance

3.4.1 Evaluation of localization performance

In this thesis, three indicators are mainly used to evaluate the performance of the localization. The three indicators are Cumulative Distribution Function (CDF), Root Mean Square Error (RMSE), Dilution of Precision (DOP).

Cumulative Distribution Function (CDF)

In order to say something about the certainty of the estimate, the CDF is used. The CDF describes the probability of the distance error being below a certain threshold and is defined as in Equation 3.1

$$F(d) = P\left\{|\hat{\mathbf{x}} - \mathbf{x}| < d\right\} \tag{3.1}$$

It is the empirical CDF that is used when evaluating the different simulations and tests with a chosen threshold of 96 %. That is, 96 % of the estimation points lies within the CDF value from the true point.

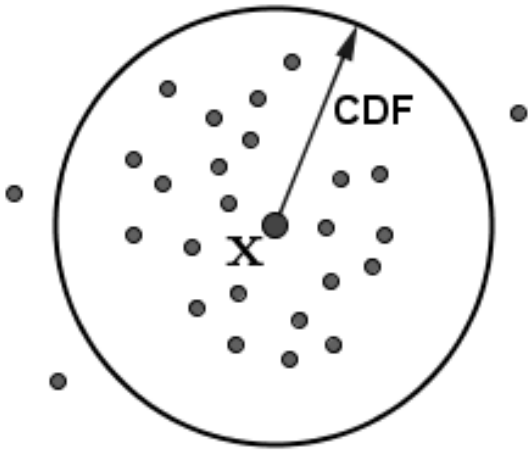

Figure 3.6: 96 % of the estimated points lie within a distance of the CDF value from the true point. The 96 & value is chosen as it corresponds to approximately two standard deviations of the normal distribution.

Root Mean Square Error

The root mean square error describes the certainty of the measurement. For zero-mean Gaussian distributed data, the RMSE corresponds to one standard deviation and defines a 68 % certainty threshold for the estimate. As it is only the the x-y coordinates this application desires, the horizontal RMSE is used. Equation 3.2 show the horizontal RMSE.

$$\begin{aligned} RMSE &= \sqrt{E[(\hat{x}-x)^2 + (\hat{y}-y)^2]} \\ &= \sqrt{\frac{1}{N}\sum_{i=1}^{N}(\hat{x}_i - x_i)^2 + (\hat{y}_i - y_i)^2} \end{aligned} \tag{3.2}$$

Dilution of Precision

The DOP or Geometric DOP is a unitless metric and describes the relation between the ranging error and position error. When the DOP value is increasing, small errors

in the ranging error leads to larger errors in the position estimate. In other words, the variance/precision of the state estimate increases.

$$DOP = \frac{\sqrt{E\left\{(\hat{\mathbf{x}} - \hat{\mu})^T(\hat{\mathbf{x}} - \hat{\mu})\right\}}}{\sigma_{range}} \tag{3.3}$$

For an unbiased estimator where, $\hat{\mu} = \mathbf{x}$, the DOP will be $DOP = \frac{RMSE}{\sigma_{range}}$. From this definition, it is seen that good geometrical conditions makes the position error less affected by the ranging error. The geometric properties in the localization system used in this thesis is mainly affected by the arrangement of the anchors.

To find the DOP values the following equation is used

$$Q = (J^T J)^{-1} \tag{3.4}$$

Where Q describes the covariance of the state estimations and J is the Jacobian of the measurement functions. The Horizontal DOP value used in this thesis is the square root of the first two diagonal elements which describes the variance in x and y direction.

The numerator on Equation 3.3 is the term for the standard deviation of the state estimator. The standard deviation describes the precision of the estimator and will be used to evaluate the localization performance. In this thesis an STD value will be the metric describing this property and is defined as seen below.

$$STD = \sqrt{\sigma_x^2 + \sigma_y^2} \tag{3.5}$$

Where σ_x^2 and σ_y^2 are the variances of the state estimate in x and y direction.

The DOP is a powerful theoretical tool when it comes to analyzing the anchor arrangement's influence on the localization performance. If the characteristics of the ranging measurements are known, it gives the ability to predict the RMSE error of the position estimate. In Figure 3.7, the DOP map of four different anchor setups can be seen.

In the DOP plot, a lower value is considered favorable. It can be seen from Figure 3.7 that placing the anchor's closely (top right) gives significantly worse geometric properties than the alternatives.

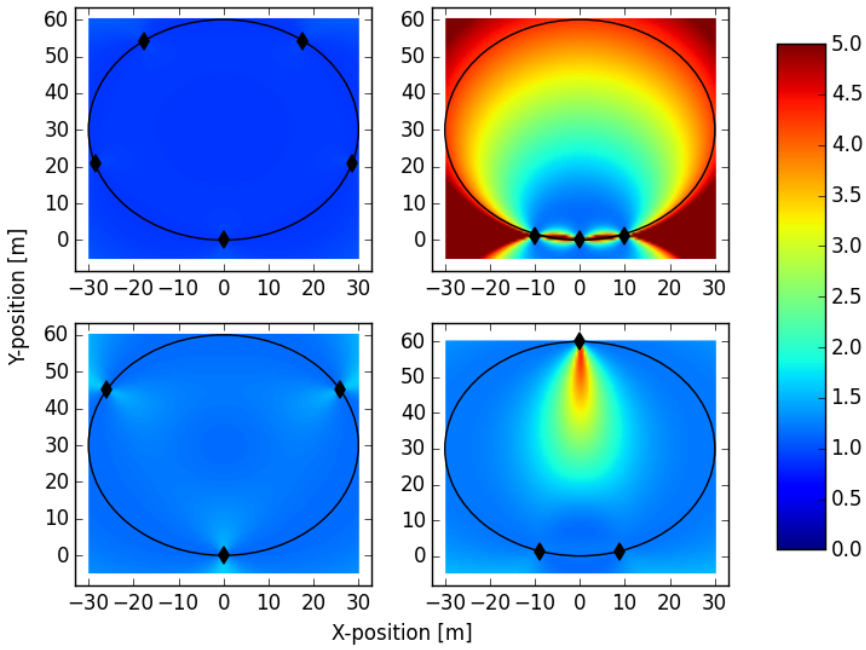

Figure 3.7: The figure shows a DOP map for different anchor (black diamonds) arrangements for round pens. The best DOP property is achieved when sensors are evenly distributed around the fish pen.

Increasing number of anchors

In [17], it is shown that the lowest possible DOP value achievable in a 2-D ranging scenario is $\frac{2}{\sqrt{N_s}}$ where N_s is the number of anchor nodes. The corresponding optimal arrangement of the anchors is to be placed in the vertices of a regular N_s sided polygon. In the upper left plot of Figure 3.7, the DOP map of a fish pen with 5 anchor nodes can be seen. From this, adding more anchors to the application could prove to be useful, but will increase the total cost of the system.

Height of anchors

The sensors' position in height have an influence on the localization performance as well. In [10, p.235], it is stated that positioning the anchors at the same height reduces the Horizontal DOP. On the other hand, placing the sensors on different levels gives better Vertical DOP values, but at the expense of the HDOP. The fence around the fish pens usually have a constant height. Placing the anchors on the fence

is considered a convenient option as it is only the horizontal coordinates of the BU that is interesting and thus a low HDOP is desired.

3.4.2 Increasing sensor distance

Figure 3.8 shows the affect of the anchor nodes' distance between each other on the localization performance. The figure shows how the RMSE changes when the distance between the remote anchors and the center anchor is increased. Figure 3.8 shows how the RMS error reduces with longer distance between the anchors. The distance in this case is not the aerial distance, but the distance along the edge of the pen. That is, the same distance as a wire potentially would have to cover. The advantage of having enough space between the anchors is substantial. However, it is important to note that the estimations in Figure 3.8 are not filtered. Filtering the results might improve the performance significantly.

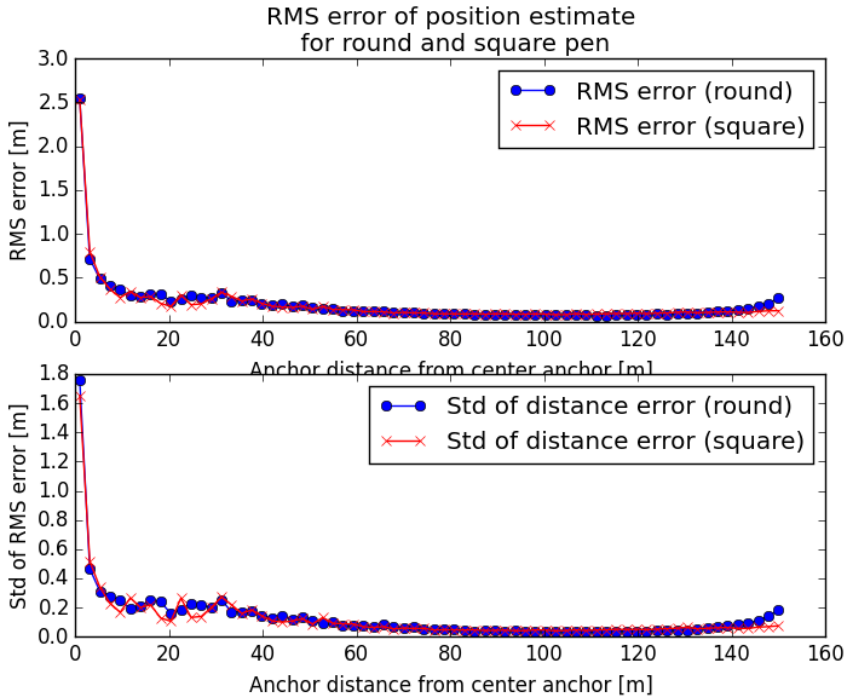

Figure 3.8: RMS error of position estimate as a function of the distance between the center anchor and the two remote anchors along fish pen edge. The round pen has a 50 meter radius and the square pen has side lengths of 50 meters. All distance measurements are normally distributed with a standard deviation of 0.1 meter. The position was estimated optimizing a Least Square problem. As seen from the plot, using current parameters need a 10 meters spacing to achieve an RMS error below 0.5 meters.

3.5 Construction of sensors

Due to the limited amount of time offered for this project, designing and development of a circuit was not done. The thesis still proposes a general idea of how such circuits could be designed.

The DW1000 modules are controlled through an SPI interface. This means that there must be a programmable controller talking to the DW1000 modules to give them instructions on how they are going to operate. The cheapest option is to use a low cost MC for this task. However, somewhere within the system, it is necessary to do certain mathematical tasks such as filtering the data. A solution to this could be to use a more powerful computer to control one of the DW1000 modules and to execute the mathematical tasks on that node. Such a computer could for instance be a Raspberry Pi. The Raspberry Pis run Linux and most are equipped with SPI support. Another advantage is that they often come with Python pre-installed and as seen in later chapters, it is Python that has been used to process the data in this thesis. This means that the same code used in the filtering algorithms made in this project can be used on the Raspberry Pis.

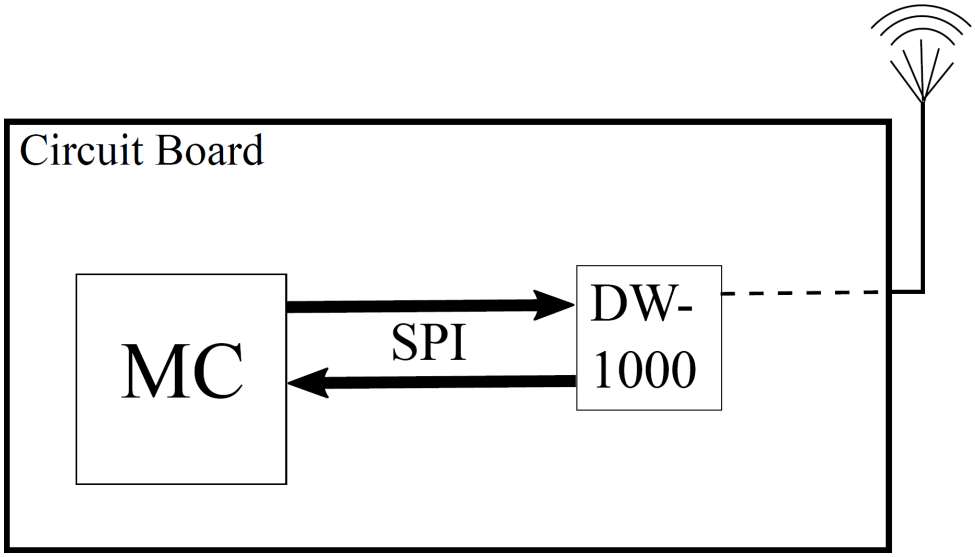

Figure 3.9: High level layout of a circuit board using the DW1000 module. The layout migh vary due to preferences from SMS.

A feasible choice would be to put the computer doing the calculations in the BU as it would mean as little information as possible would need to be exchanged between the nodes. As the DW1000 IC supports TWTOF, the BU node will only need to measure its distance to the three anchor nodes which will only have the

task to reply to the ranging messages that they receive. Another advantage using Raspberry Pi is that it has other means of communications available than SPI as well. Ethernet or Universal Series Bus (USB) are such options. This gives the localization system several ways of integrating into the rest of SMS' system.

Chapter 4
State Estimation and Filtering

This chapter describes various filters and data processing techniques that are used in this project.

4.1 Least Square Estimator (LSE)

One way of estimating the position of the buoy is using a Least Square Estimator (LSE). It has the advantage of not needing any prior information about the system. The LSE estimates the states by minimizing a cost function. This cost function is the sum of the squared errors between the measurements and the corresponding measurement functions. The formulation of the problem is seen in Equation 4.1.

$$\hat{\mathbf{x}}^{\mathbf{b}} = \arg\min_{\mathbf{x}^{\mathbf{b}}} \sum_{i=1}^{N_m} (z_i - f_i(\mathbf{x}^{\mathbf{b}})) \tag{4.1}$$

Where z_i is measurement i and f_i is the corresponding measurement function. In the case of ranging, the measurement function will be the distance between $\mathbf{x}^{\mathbf{b}}$ and anchor i. A graphical illustration of the problem can be seen in Figure 4.1. In [10], it is shown that when assuming an additive zero mean Gaussian error in the measurement, this is the maximum likelihood (ML) solution of the problem. That is, the most likely position of $\mathbf{x}^{\mathbf{b}}$ given the measurements. The LSE can also be applied in a recursive manner where states from previous time steps are used as well when estimating current state. In the recursive case, earlier states will be weighted less and more recent states weighted higher. This project does not use the recursive LSE, but uses another recursive filter instead, the Kalman filter (KF).

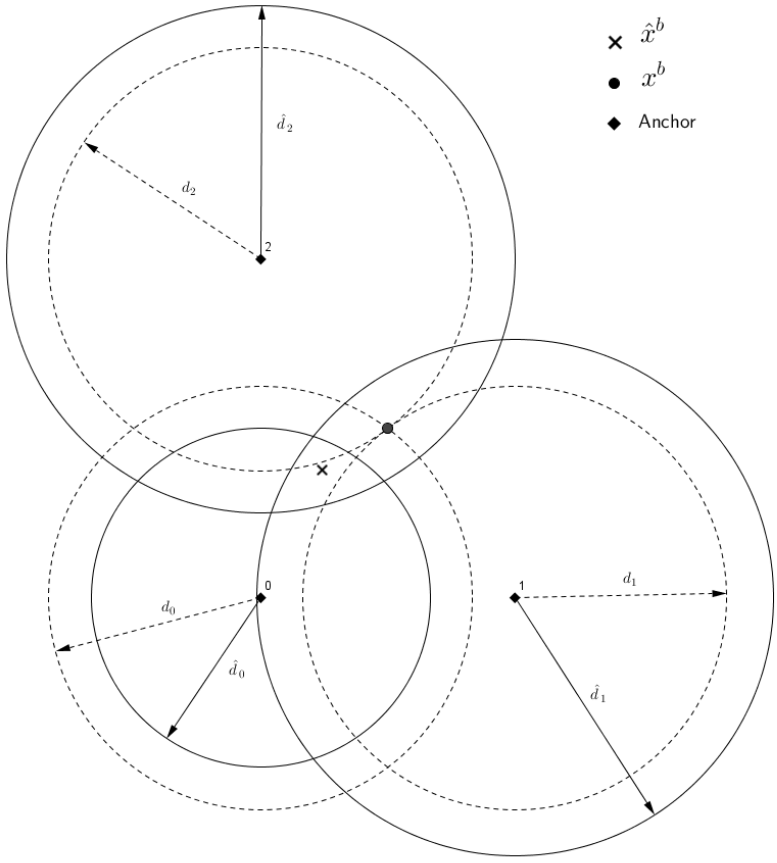

Figure 4.1: Trilateration using a LSE. Due to the measurement errors, there is no single corresponding point where all three circles intersect. Instead, a solution that minimizes the sum of squared distances from the estimated state to each circle arc is found.

Gauss Newton Algorithm

Problems on the form seen in Equation 4.1 are not always possible to solve analytically, especially if the measurement function is non-linear. This means that a numerical approach needs to be taken. A common numerical approach to use on least square (LS) problems is the Gauss Newton Algorithm. The Gauss Newton algorithm uses the Jacobian ($\mathbf{H}(\mathbf{x})$) of the measurement function ($\mathbf{h}(\mathbf{x})$) to find the gradient of the error function. The algorithm can be seen below.

Algorithm 4.1 The Gauss Newton Algorithm

$i \leftarrow 0$
$\alpha_0 \leftarrow 1$
while $V(\hat{\mathbf{x}}_\mathbf{0}) <$ minimum error **or** $i >$ maximum iterations **do**
  $\hat{\mathbf{x}}_{\mathbf{i+1}} \leftarrow \hat{\mathbf{x}}_\mathbf{i} + \alpha_i(\mathbf{H}(\hat{\mathbf{x}}_\mathbf{i})^T\mathbf{H}(\hat{\mathbf{x}}_\mathbf{i}))^{-1}\mathbf{H}(\hat{\mathbf{x}}_\mathbf{i})^T(\mathbf{z} - \mathbf{h}(\hat{\mathbf{x}}_\mathbf{i}))$
  if $V(\hat{\mathbf{x}}_{\mathbf{i+1}}) > V(\hat{\mathbf{x}}_i)$ **then**
    $\alpha_i \leftarrow \frac{\alpha_i}{2}$
  else
    $i \leftarrow i + 1$
    $\alpha_{i+1} \leftarrow 1$
  end if
end while

4.2 The Kalman filter

The following section describes the Discrete Kalman filter algorithm. Most of the information is gathered from [11]. However, the notation differs as it befits the author of this thesis.

The Kalman filter is a special case of the Bayesian filter. It assumes a discrete linear system with additive Gaussian white noise and is proven to be optimal and unbiased if these assumptions hold.

The Kalman filter requires a formulation of the system on the following form.

$$\mathbf{x}_k = \mathbf{A}_k\mathbf{x}_{k-1} + \mathbf{w}_k \tag{4.2}$$

Where $\mathbf{x}_k$ is the system states at iteration step k and $\mathbf{w}_k$ is Gaussian white-noise with known covariance. $\mathbf{A}_k$ is the state transition matrix at time k. Further, the output or measurements of the system is on the form

$$\mathbf{z}_k = \mathbf{H}_k\mathbf{x}_k + \mathbf{v}_k \tag{4.3}$$

Where $\mathbf{H}_k$ gives the linear connection between the states and the measurements and $\mathbf{v}_k$ is the white measurement noise at time k. An important assumption is that $\mathbf{w}_k$ and $\mathbf{v}_k$ are uncorrelated to other time steps and are uncorrelated to each other as described in equation 4.4

$$
\begin{aligned}
E[\mathbf{w}_k \mathbf{w}_k^T] &= \begin{cases} \mathbf{Q}_k & , i = k \\ \mathbf{0} & , i \neq k \end{cases} \\
E[\mathbf{v}_k \mathbf{v}_k^T] &= \begin{cases} \mathbf{R}_k & , i = k \\ \mathbf{0} & , i \neq k \end{cases} \\
E[\mathbf{w}_k \mathbf{v}_k^T] &= \mathbf{0}, \ \forall k, i
\end{aligned} \tag{4.4}
$$

The Kalman filter, as other Bayesian Filters, consists of two steps, a prediction step and an update step. The principle works in the following way. First, use known transitional relations to project ahead and predict next step. Then do measurements and merge probability distributions to find the most likely position of $\mathbf{x}$. The Kalman filter has two variables it predicts and updates, the states of the system $\mathbf{x}$ and the error covariance matrix $\mathbf{P}$.

The prediction step is as described in the steps under (4.5) and gives a prior knowledge of the estimate. The variables with subscript $k|k-1$ are hence called prior variables.

$$
\begin{aligned}
\hat{\mathbf{x}}_{k|k-1} &= \mathbf{A}_k \hat{\mathbf{x}}_{k-1|k-1} \\
\mathbf{P}_{k|k-1} &= \mathbf{A}_k \mathbf{P}_{k-1|k-1} \mathbf{A}_k + \mathbf{Q}_k
\end{aligned} \tag{4.5}
$$

The prediction step uses the estimates of the previous step to predict the most likely state ($\hat{\mathbf{x}}$) and associate error covariance matrix $\mathbf{P}$. After the prediction step follows the update step. The update step uses information from the prediction step and measurements to find the most likely estimate of $\mathbf{x}$. Using the two prior variables calculated in the prediction step along with the measurement matrix ($\mathbf{H}$) and its error covariance matrix ($\mathbf{R}$) an optimal gain can be derived. The optimal gain ($\mathbf{K}$) will have the following form.

$$
\mathbf{K}_k = \mathbf{P}_{k|k-1} \mathbf{H}_k^T (\mathbf{H}_k \mathbf{P}_{k|k-1} \mathbf{H}_k^T + \mathbf{R}_k)^{-1} \tag{4.6}
$$

The optimal gain is used to merge the prior estimate of $\mathbf{x}$ with the measurements ($\mathbf{z}$) at time k. The merge of these two is done in the way described in equation 4.7 below.

$$
\hat{\mathbf{x}}_{k|k} = \hat{\mathbf{x}}_{k|k-1} + \mathbf{K}_k (\mathbf{z}_k - \mathbf{H}_k \hat{\mathbf{x}}_{k|k-1}) \tag{4.7}
$$

As a new estimate of $\mathbf{x}$ is now computed, the error covariance matrix has to be updated as well. This is shown in equation 4.8.

$$\mathbf{P}_{k|k} = (\mathbf{I} - \mathbf{K}_k\mathbf{H}_k)\mathbf{P}_{k|k-1} \tag{4.8}$$

$\mathbf{x}_{k|k}$ and $\mathbf{P}_{k|k}$ are called the posterior variables as they have taken the measurement data into account as well. This concludes the recursive Kalman filter algorithm for time step k.

When it comes to initializing the Kalman filter, it is required to have an initial state $\mathbf{x}_{0|0}$ and the corresponding covariance matrix $\mathbf{P}_{0|0}$. If the exact initial position of $\mathbf{x}_{0|0}$ is known $\mathbf{P}_{0|0}$ is a zero-matrix. The practical performance of the Kalman filter depends on how well the model fits the real world.

4.2.1 The Extended Kalman filter

As most systems in the world today are non-linear, the Kalman filter needs a way to handle non-linear problems. This is where the Extended Kalman filter comes in.

Rewrite the system equations 4.2 and 4.3 to be on the form.

$$\mathbf{x}_k = f(\mathbf{x}_{k-1}) + \mathbf{w}_k \tag{4.9}$$

$$\mathbf{z}_k = h(\mathbf{x}_k) + \mathbf{v}_k \tag{4.10}$$

Where $\mathbf{w}$ and $\mathbf{v}$ are the same noise processes with the same properties as in the linear case. This formulation allows $f(\mathbf{x}_{k-1})$ and $h(\mathbf{x}_k)$ to be non-linear functions. In order to make this work with the linear Kalman filter Algorithm the system is linearized. This makes the $\mathbf{A}$ and $\mathbf{H}$ matrices on the following form.

$$\mathbf{A}_k = \left.\frac{\partial f}{\partial \mathbf{x}}\right|_{\hat{\mathbf{x}}_{k-1|k-1}} \tag{4.11}$$

$$\mathbf{H}_k = \left.\frac{\partial h}{\partial \mathbf{x}}\right|_{\hat{\mathbf{x}}_{k|k-1}} \tag{4.12}$$

The steps of the algorithm is executed in almost the same way as in the linear case, but the updates of the prior and posterior estimate of $\mathbf{x}$ are slightly different.

Instead of using the linearized $\mathbf{A}$ and $\mathbf{H}$ when updating $\mathbf{x}$, the nonlinear equations in 4.9 and 4.10 are used instead. This makes the update of the prior and posterior estimate of $\mathbf{x}$ to be on the form seen in equations 4.13 and 4.14 respectively.

$$\hat{\mathbf{x}}_{k|k-1} = f(\hat{\mathbf{x}}_{k-1|k-1}) \tag{4.13}$$

$$\hat{\mathbf{x}}_{k|k} = \hat{\mathbf{x}}_{k|k-1} + \mathbf{K}_k(\mathbf{z}_k - h(\hat{\mathbf{x}}_{k|k-1})) \tag{4.14}$$

The rest of the steps of the algorithm are identical to the linear case. Unlike the linear filter, the Extended Kalman filter is not optimal. Because of the linearization, the filter is more unpredictable and might diverge from the true $\mathbf{x}$ value. This is especially the case if the measurements are noisy or the initialization of the algorithm is inaccurate.

4.3 Determining anchor positions

A crucial factor to get a good position estimate is how well the parameters of the measurement model fits the parameters of the real system. More specifically, these parameters are the position of the anchors. One could standardize the anchor positions and say that they should always have the same distance between them (e.g 20 meters). Then the burden of making the anchor positions sufficiently accurate lays on the people setting up the system. The biggest disadvantage using this approach is the rigidity of such a solution. Not all fish pens are the same and not having any flexibility when positioning the anchors leaves a bigger risk of interfering with other operations on the location. An alternative to this approach is setting the sensors up in a convenient way for every single pen, then manually measure the positions of the anchors and feed the parameters into the localization algorithms. This is a good alternative, but still relies heavily on the crew setting up the system.

Routine for self calibrating anchors

A third way is letting the system calibrate itself. The UWB modules already have the possibility to do ranging measurements between them and this information could be used to estimate the anchor positions. Letting the system find the anchor positions by itself would be convenient as it would reduce the workload of the workers setting up the system and give flexibility regarding where to put the anchors.

As the anchors are located on the edge of the pen, certain geometrical properties can be used to estimate the anchor positions. For instance, in a circular pen, the distance from the anchor to the center of the pen is equal to the radius of the pen.

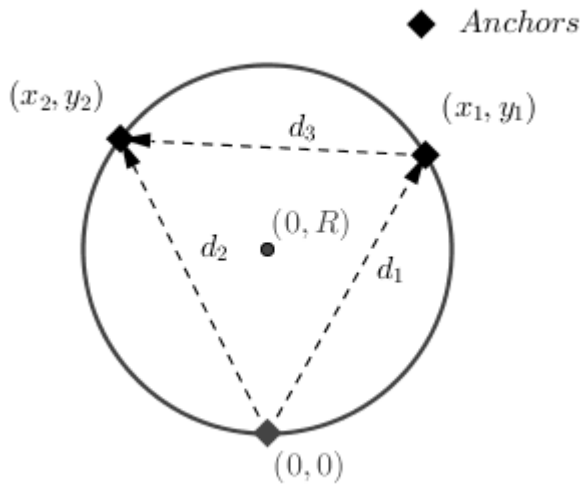

Figure 4.2: A graphical view of the anchor estimation scheme in a circular pen. For each remote anchor is it only necessary to know the distance to the center anchor, but a third measurement between the two remote anchors could give a higher accuracy.

Additionally, by including the equation for the square distance from the center anchor to the remote anchor you get two equations.

$$x_i^2 + (y_i - R)^2 = R^2 \tag{4.15}$$
$$x_i^2 + y_i^2 + z_i^2 = d_i^2 \tag{4.16}$$

By subtracting Equation 4.15 from Equation 4.16 and solve for y_i you get

$$y_i = \frac{d_i^2 - z_i^2}{2R} \tag{4.17}$$

which can be plugged back into Equation 4.16 to get the following equation for x_i

$$x_i = \pm\sqrt{d_i^2 - (\frac{d_i^2 - z_i^2}{2R})^2 - z_i^2} \tag{4.18}$$

The sign of x_i can be chosen with prior information about which side of the center anchor the remote anchor is on. That is, if it's on the left, pick the negative sign and if it's on the right, pick the positive sign. Equations 4.17 and 4.18 offers an analytical solution to the problem as long as $0 <= d_i <= 2R$. If the position of the anchor is at the opposite side of the circle from the center anchor, the measurements could be greater than $2R$. This could be solved by clamping the measurements to the interval $[0, 2R]$.

A third measurement between the two remote anchors could also be added to include more information. The relation of the two remote anchors and the distance between them is expressed in Equation 4.19.

$$(x_1 - x_2)^2 + (y_1 - y_2)^2 = d_3^2 \tag{4.19}$$

Adding the third distance measurement removes the opportunity to solve the problem analytically and thus require a numerical solution instead. The problem can be solved as another LS problem on the following form

$$\hat{\theta} = \arg\min_{\hat{\theta}} \left[\sum_{i=1}^{2} \left(\epsilon_i(\hat{\theta}, \hat{d}_i)^2 + \xi_i(\hat{\theta}, \hat{d}_i)^2 \right) + \varphi(\hat{\theta}, \hat{d}_3)^2 \right] \tag{4.20}$$

$$\hat{\theta} = \begin{bmatrix} x_1 \\ y_1 \\ x_2 \\ y_2 \end{bmatrix}$$

$$\epsilon_i(\hat{\theta}, \hat{d}_i) = \sqrt{2y_i R + z_i^2} - \hat{d}_i$$

$$\xi_i(\hat{\theta}, \hat{d}_i) = \sqrt{x_i^2 + y_i^2 + z_i^2} - \hat{d}_i$$

$$\varphi(\hat{\theta}, \hat{d}_3) = \sqrt{(x_1 - x_2)^2 + (y_1 - y_2)^2} - \hat{d}_3$$

A more thorough explanation on solving this problem is given in section 6.3.

Figure 4.3 shows that the difference between the numerical and analytical solutions is minor. With no error in the measurement, both the analytical and the numerical solution will provide a perfect estimate of the anchor positions. For really small errors in the measurements, the two estimates will have almost the exact same error. That the numerical solution does not help a lot if the error in the measurement is

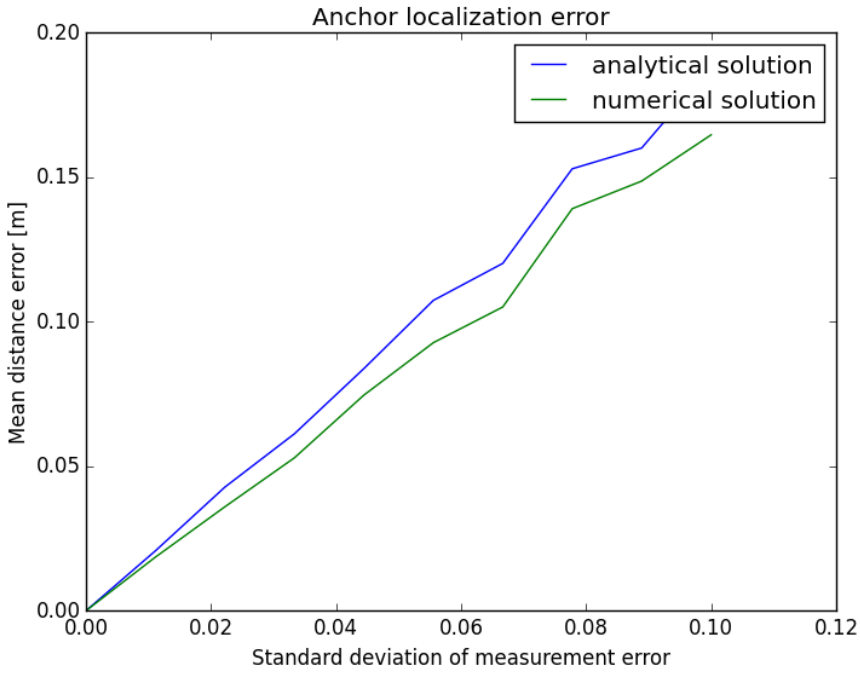

Figure 4.3: This plot shows the mean distance error when solving the LS-problem in Equation 4.20 and the analytical solution in Equation 4.17 - 4.18. It shows the error plotted against different values of the noise parameters (standard deviation of zero-mean Gaussian noise). The remote anchors are randomly positioned on the edge of the circle and the error is averaged over 500 samples for each value of the noise parameters.

small is unsurprising. After all, the numerical solution was introduced to reduce the influence of the measurement error. However, the numerical solution seems to perform better when the measurement error becomes bigger, so adding a third measurement can seem like a good idea. Another way of reducing the error is averaging the distance measurements. As the standard deviation of the mean of a random variable is inversely proportional to the square root of the number of samples (n). If the calibration routine gets enough time, n will be so large the measurement error will be almost insignificant. This assumes that there are no bias in the measurements.

Calculating a numerical solution will in most cases be more time consuming and computationally expensive than computing the analytical equations. This is due to the iterations required in the gauss newton algorithm. The node on the BU will have a more powerful computer than the anchors and is a natural choice to

do the computations. Most likely, the computer on the BU will be fast enough to solve the numerical solution without any significant delay. A more important factor that might cause large problems regarding the performance of this routine is the assumption made in Equation 4.15. That is, the assumption that the fish pen is a perfect circle. It was discussed earlier that due to various reasons, such as weather, it is possible that the fish pens deform. This means that the weather conditions must be appropriate when calibrating the system. Even with perfect weather conditions, it is a bold assumption that the pen is a perfect circle and it is hard to say whether this estimation routine will perform satisfyingly when applied to a real world system. This is left to be tested in a later part of this project.

Chapter 5
Test Cases

In order to verify whether a system using UWB ranging sensors is feasible, several tests were carried out. The different tests had to reflect what was considered to be the theoretical and practical challenges with using a UWB ranging system. This spans from tests validating the performance of the different localization algorithms to verifying the sensors' characteristics and behavior in environments similar to the environment on the BU. This lead to the following test cases.

Case 1: Validation of sensor error model

Case 2: Small and large pen with surrounding anchors

Case 3: Small and large pen with displaced anchors

Case 4: Anchors positioned on line with short and longer distance

Case 5: Test sensors near water

Case 6: The tag is blocked with POM

A more thorough explanation of the cases and their motivation follows below. It was considered useful to simulate case 2 - 4 to examine the theoretical performance of the Extended Kalman Filter (EKF) and LSE and what results to expect in the field tests. The result of these simulations can be found in chapter 7. As case 1, 5 and 6 are testing the practical behavior of the sensors, it was considered unnecessary to simulate them.

5.1 Case 1: Validation of sensor error model

DecaWave state in the DW1000's data sheet[1] that the typical ranging error is a zero-mean Gaussian distribution with a standard deviation of 2 centimeter. These

claims had to be validated as the error model was used in the simulations (an assumption when using a Kalman filter (KF)), and considered a valuable knowledge when examining the theoretical abilities of the system. More on how the tests were conducted and the results are found in section 8.2.

5.2 Case 2: Small and large pen with surrounding anchors

Before potentially implementing a system using the DW1000 sensors, it was necessary to examine the localization abilities of different configurations of the system. The test was set up to reflect how the system anchors could be expected to perform with the anchors surrounding the tag. The configuration was simulated before the tests took place to look into the theoretical possibilities regarding the localization performance and verifying the suitability of using an EKF and a LSE. Typically, round fish pens in Norway have a circumference of either 120 or 160 meter which corresponds to diameters of approximately 38 and 57 meters respectively. In order to examine the localization performance of both pen types, the test case was divided into two parts. Part **a** would reflect the smaller fish pen and part **b** the larger.

5.3 Case 3: Small and large pen with displaced anchors

As discussed in subsection 3.1.1, the round pens might become disfigured due to external forces acting on them. Such disfiguring would change the remote anchors' position relative to the center anchor. Case 3 examines the case where the estimators uses the wrong position of the remote anchors. It is a special case of case 2 and uses the same node setup. This case was not tested in the field tests as it was set up to theoretically examine the behavior of the system with displaced anchors.

5.4 Case 4: Anchors placed on line with short and longer distance

Subsection 3.3.2 discusses alternatives to distributing the anchors in a surrounding manner. Due to practical considerations, it was proposed to put the anchors closely. However, positioning the anchors closely gives the system poor geometric properties. Case 4 examines the localization performance under such conditions. The case was simulated before the tests were done to possibly exclude the inclusion of such a configuration in the field test cases and to see what performance that could be expected.

Just as with case 2, case 4 consists of two parts. Part **a** uses a short distance between the anchors and part **b** have a longer distance.

5.5 Case 5: The sensors' behavior in the proximity of water

Because of the of water's tendency to either absorb or reflect RF signals, RF equipment in marine applications with a short distance to the water are occasionally experiencing a poor performance. The BU is floating in the water surface and it is necessary that the ranging sensors are capable of coping with such conditions. This was a crucial test for the suitability of the DW1000 ICs for this application. If the test indicated that the IC was unfit to be used in the proximity of water, using the the DW1000 IC to localize the BU would not be a feasible option.

5.6 Case 6: POM blocking of tag

It is desired to place the BU sensor and antenna inside the lid of the BU which is made of Polyoxymethylene (POM). The sensor working with the antenna inside the lid would be advantageous as there would be no need to drill a hole in the lid for the antenna. To examine the sensors' penetrating ability, tests were carried out where the tag was covered by a various number of POM plates. The test for Case 6 was done in combination with Case 5.

Chapter 6
System Models

6.1 Model of Buoy

Even though the buoy will be located on the water surface and it is only the x-y coordinates that are interesting, the z-coordinate is included in the buoy model. This is because the sensors are likely to be placed at some distance above the water surface and the distance in z-direction will be included in the measurements. If the buoy had a constant height the z-coordinate could have been discarded as the measurements could have been corrected by subtracting the z-component. However, the buoy's z-position will fluctuate due to waves and is therefor included in the model.

$$\mathbf{x^b} = \begin{bmatrix} x^b \\ y^b \\ z^b \end{bmatrix} \tag{6.1}$$

The buoy is strapped to a wire that causes its position to be almost stationary. Due to forces from the water its position will vary slightly. This is described by the noise components v_n.

$$\mathbf{x^b_{n+1}} = \underbrace{\begin{bmatrix} 1 & 0 & 0 \\ 0 & 1 & 0 \\ 0 & 0 & 0 \end{bmatrix}}_{A} \mathbf{x^b_n} + \begin{bmatrix} v_n^x \\ v_n^y \\ v_n^z \end{bmatrix} \tag{6.2}$$

An alternative error model could be to describe the buoy movement as a random walk along the wire it is strapped to. To be able to model the buoy that way additional information about the setup of the wire would be needed. This is information that is not available. It could be measured when installing the system, but to keep the

system flexible the workers on the fish farm should be able to change the mounting point of the wire without having to recalibrate the parameters of the localization algorithm. As the wire is not necessarily completely stretched out either, designing the model to use the wire seems unnecessary. The z-coordinate is assumed to have a zero-mean position with a Gaussian disturbance caused by waves.

6.1.1 Ranging model

To investigate how the ranging precision affects the overall localization result and to see how other parameters affect the system, a model of the range measurements was made. The following model has been used to generate measurements.

$$h_i = \sqrt{(x^b - x_i^a)^2 + (y^b - y_i^a)^2 + (z^b - z_i^a)} + w \tag{6.3}$$

Where x_i^a, z_i^a and z_i^a are the x, y and z positions of anchor i and h_i is the distance measurement from the buoy to anchor i. x^b, y^b and z^b are defined in Equation 6.1. w is zero-mean additive Gaussian noise. The model is backed up by the data sheet of the DW1000 module[1].

6.2 Kalman Filter Model

In the model of the buoy described above (6.2), the buoy is assumed to be stationary apart from a random disturbance causing it to move. This makes the update step of $\mathbf{x_{n|n-1}}$ as described in 6.4. Where A is the state propagation matrix.

$$\mathbf{x_{n|n-1}} = \underbrace{\begin{bmatrix} 1 & 0 & 0 \\ 0 & 1 & 0 \\ 0 & 0 & 0 \end{bmatrix}}_{A} \mathbf{x_{n-1|n-1}} \tag{6.4}$$

The disturbance working on the buoy in x and y direction are assumed to be uncorrolated. Using this assumption $\mathbf{Q}$ can be chosen as in 6.5.

$$\mathbf{Q} = \begin{bmatrix} q_1 & 0 & 0 \\ 0 & q_2 & 0 \\ 0 & 0 & q_3 \end{bmatrix} \tag{6.5}$$

In the same way as $\mathbf{Q}$, $\mathbf{R}$ can be chosen as well.

$$\mathbf{R} = \begin{bmatrix} r_1 & 0 & 0 \\ 0 & r_2 & 0 \\ 0 & 0 & r_3 \end{bmatrix} \tag{6.6}$$

Choosing $\mathbf{Q}$ and $\mathbf{R}$ to be diagonal matrices assumes the random variables of the system to be independent. In the case of the measurement covariance, this is a fair assumption because of the independence of each range measurement. There is no data available to examine the movement of the BU. This makes it difficult to assume whether the covariance is a diagonal matrix or not. One could argue that because of the wire that the BU is connected to, q_1 and q_2 would be correlated in some way, but that idea is discarded as the opposite could just as well be the case and there is no available movement data to support that claim. As q_3 describes the uncertainty in the z-direction and therefore functions as a model of the waves.

As described in Section 4.2.1, the extended Kalman Filter needs functions to describe the relationship between the system's states and the measured value. As the measured value is the distance between each anchor node and the tag node, these measure functions can be described as below.

$$\mathbf{h}(\mathbf{x}) = \begin{bmatrix} h_1 \\ ... \\ h_m \end{bmatrix} \tag{6.7}$$

Where

$$h_i(\mathbf{x}) = \sqrt{(x^b - x_i^a)^2 + (y^b - y_i^a)^2 + (z^b - z_i^a)^2} \tag{6.8}$$

Where x_i^a and y_i^a are the x and y positions of anchor i and h_i is the measurement from the buoy to anchor i.
From this the linearized measurement matrix $\mathbf{H}$ is derived.

$$\mathbf{H}(\mathbf{x}) = \begin{bmatrix} \frac{x^b - x_1^a}{h_1(\mathbf{x})} & \frac{y^b - y_1^a}{h_1(\mathbf{x})} & \frac{z^b - z_1^a}{h_1(\mathbf{x})} \\ ... & ... & ... \\ \frac{x^b - x_m^a}{h_m(\mathbf{x})} & \frac{y^b - y_m^a}{h_m(\mathbf{x})} & \frac{z^b - z_m^a}{h_m(\mathbf{x})} \end{bmatrix} \tag{6.9}$$

The variables described above are then used in the Extended Kalman Filter algorithm as described in Section 4.2.1.

6.3 Anchor position estimation

As shown in section 4.3 can the problem of finding the position of the anchors be formulated as a LS problem. If it's assumed that the z-position (height) of each sensor is known. After all, this is an easy demand to fulfill as the sensors can be mounted on the fence surrounding the fish pen as well as on the available locker. This leaves four unknown states to estimate (Equation 6.10).

$$\theta = \begin{bmatrix} x_1 \\ y_1 \\ x_2 \\ y_2 \end{bmatrix} \tag{6.10}$$

The LS problem has to be solved numerically due to the non-linearities in the measurement functions in Equation 6.11

$$\mathbf{z} = \mathbf{h}(\theta) = \begin{bmatrix} \hat{d}_1 \\ \hat{d}_2 \\ \hat{d}_1 \\ \hat{d}_2 \\ \hat{d}_3 \end{bmatrix} = \begin{bmatrix} \sqrt{2y_1R} \\ \sqrt{2y_2R} \\ \sqrt{x_1^2 + y_1^2 + z_1^2} \\ \sqrt{x_2^2 + y_2^2 + z_2^2} \\ \sqrt{(x_1^2 - x_2^2)^2 + (y_1^2 - y_2^2)^2} \end{bmatrix} \tag{6.11}$$

To do this, the Gauss Newton algorithm described in section 4.1 can be applied. The Gauss Newton algorithm uses the Jacobian of the measurement function to find the minimum of the LS problem. The Jacobian is shown in Equation 6.12.

$$\mathbf{H}(\theta) = \begin{bmatrix} 0 & \frac{R}{\sqrt{2y_1R}} & 0 & 0 \\ 0 & 0 & 0 & \frac{R}{\sqrt{2y_1R}} \\ \frac{x_1}{\sqrt{x_1^2+y_1^2}} & \frac{y_1}{\sqrt{x_1^2+y_1^2}} & 0 & 0 \\ 0 & 0 & \frac{y_2}{\sqrt{x_2^2+y_2^2}} & \frac{y_2}{\sqrt{x_2^2+y_2^2}} \\ \frac{x_1}{\phi(\theta)} & \frac{y_1}{\phi(\theta)} & -\frac{x_2}{\phi(\theta)} & -\frac{y_2}{\phi(\theta)} \end{bmatrix} \tag{6.12}$$

$$\phi(\theta) = \sqrt{(x_1 - x_2)^2 + (y_1 - y_2)^2}$$

By using the following matrices and the Gauss Newton algorithm an optimal solution to the anchor localization problem is found. The simulations show how the

anchor localization performs with different noise parameters. More specifically, it's the standard deviation of the zero-mean Gaussian noise that is altered. For each noise parameter are the anchors position randomly on the edge of the fish pen and the result is averaged over N different anchor positions. The results of the simulations made to test this algorithm can be found in section 4.3.

Chapter 7
Simulations

Before conducting the field tests, some simulations were made to get an indicator of the localization performance that could be expected when conducting the field tests. This chapter describes the simulations and discusses the results obtained. All source code is found in the digital appendix and a short description is included in Appendix B

7.1 Framework

When deciding on which tools to use for data processing and simulations, the available resources of SMS had to be taken into account. MATLAB is commonly used in academic work and by companies that needs user friendly simulation tools, but as their licenses are expensive is it not a suitable program for all companies. Luckily, there are available free options as well. Python have a great number of free and open source libraries available, and some of them can replace a lot of the functionality MATLAB offers. Numpy [5], Matplotlib [4] and Scipy [9] are examples of this. Even though they are not as user friendly and intuitive as MATLAB, the transition from MATLAB to these libraries is uncomplicated. Numpy offers array and matrix structures with convenient functionality such as statistical properties (e.g mean and standard deviation) and linear algebra operations. Scipy offers scientific computing tools such as optimization functions, while Matplotlib offers plotting tools. The data processing and simulations made in this thesis are implemented in Python using said libraries.

7.2 Simulation of case 2

Before testing the sensors in the real world, the localization algorithms were simulated to get an indication of what to expect. Different sensor setups were tested and having prior assumptions of the estimators' behavior was useful. It gave indications on

which estimator that would be the best choice and showed the theoretical abilities of the localization system.

In section 3.4.1, it was stated that the anchor arrangement that gives the best DOP properties is when they are evenly distributed around the pen. However, due to practical considerations when doing the field tests later, the anchors were corners in an isosceles triangle instead. Two different configurations were simulated. One simulation for a large fish pen and one for a small fish pen.

7.2.1 Simulation setup

A sketch of the setup can be seen in Figure 7.1. The two parameters L and L_y could be varied to change the size of the pen. To make the setup in the simulation similar to the setup that was intended for the experimental tests, the values of the parameters had to be chosen accordingly. The experimental tests were to take place on a football field and intended to use appropriate lines and markings that existed on the field. To make the setup fit said markings, the base line was chosen to have a length of 21.0 meters ($L = 21$) for both configurations. L_y was given the lengths 33.6 and 67.2 which corresponds to fish pens with radius 18.4 and 34.4 meters respectively.

The measurements were simulated to have a zero-mean Gaussian error with a standard deviation of 5 centimeters. The buoy had a mean position of $(10.5, 18.0, 0.0)$ and small zero-mean Gaussian noise with standard deviation of five centimeters was added to the BU as well to emulate the small movements caused by waves.

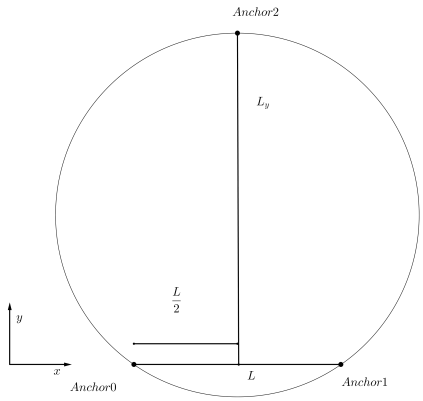

Figure 7.1: The Figure shows a sketch of the setup that was simulated. Two anchors would make up the base line and the last anchor would be positioned at the other end in the middle.

7.2.2 Results

	LS (large)	LS (small)	KF (large)	KF (small)
CDF [m]	0.159	0.194	0.079	0.067
RMSE [m]	0.080	0.087	0.043	0.038
STD [m]	0.074	0.086	0.038	0.034
Mean error (x)	0.037	0.027	0.000	-0.007
Mean error (y)	-0.007	0.005	-0.010	-0.005

Table 7.1: The Table shows some statistical values for the simulations of case 2. The KFs performed significantly better than the LSEs

The results of the simulation is found in Figure 7.3 and 7.2 along with statistical values in Table 7.1. The Figures show how the KFs' performance is superior to the performance of the LSEs. The CDF values of the KFs are less than half of what the LSEs offers. These results are significant and show the potential benefit of using a KF to improve the data filtering. When also considering the STD being under half of the LSEs', the KFs seems a superior choice.

Using the KFs is only valid if the model used is similar enough to the BU's behavior in the real world. That is, the measurement noise is zero-mean Gaussian distributed and the BU's position is more or less constant except for a varying disturbance due to waves. Whether this assumption will hold in a real fish pen is hard to conclude on, but available videos[22] indicates that the assumption is fair.

Table 7.1 shows that all estimators are unbiased. This is very beneficial as it means that the state estimations are evenly distributed around the true value.

A 96 % chance of the estimate being within 8 centimeters for both pen configurations was well within the desired performance for the application. Even the LSEs had a CDF value of about 20 centimeters which is accepted as well. The simulation results showed the potential benefits of placing the sensors in a triangle that spans the pen. With the promising results of the simulations, it was decided to proceed with field tests for Case 2.

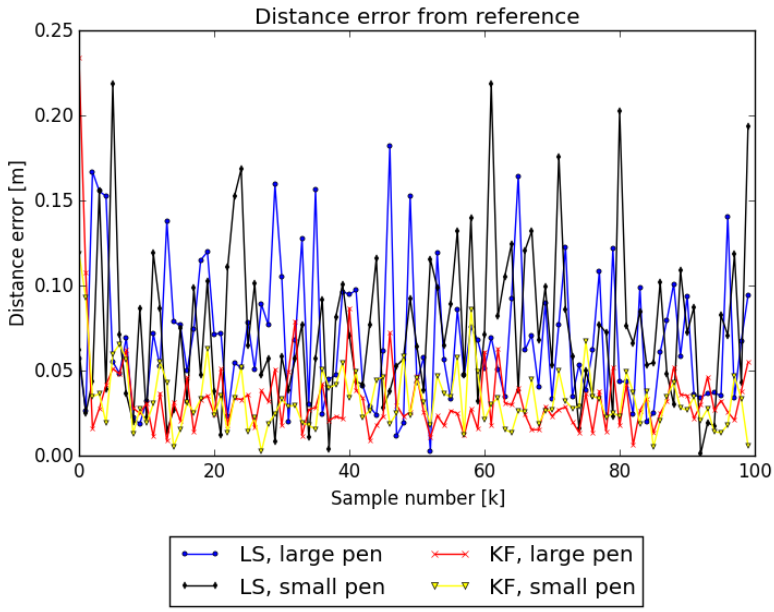

Figure 7.2: The top figure shows how well the estimators follow each state and shows that the accuracy is high for both. The lower figure shows the distance errors for each time step.

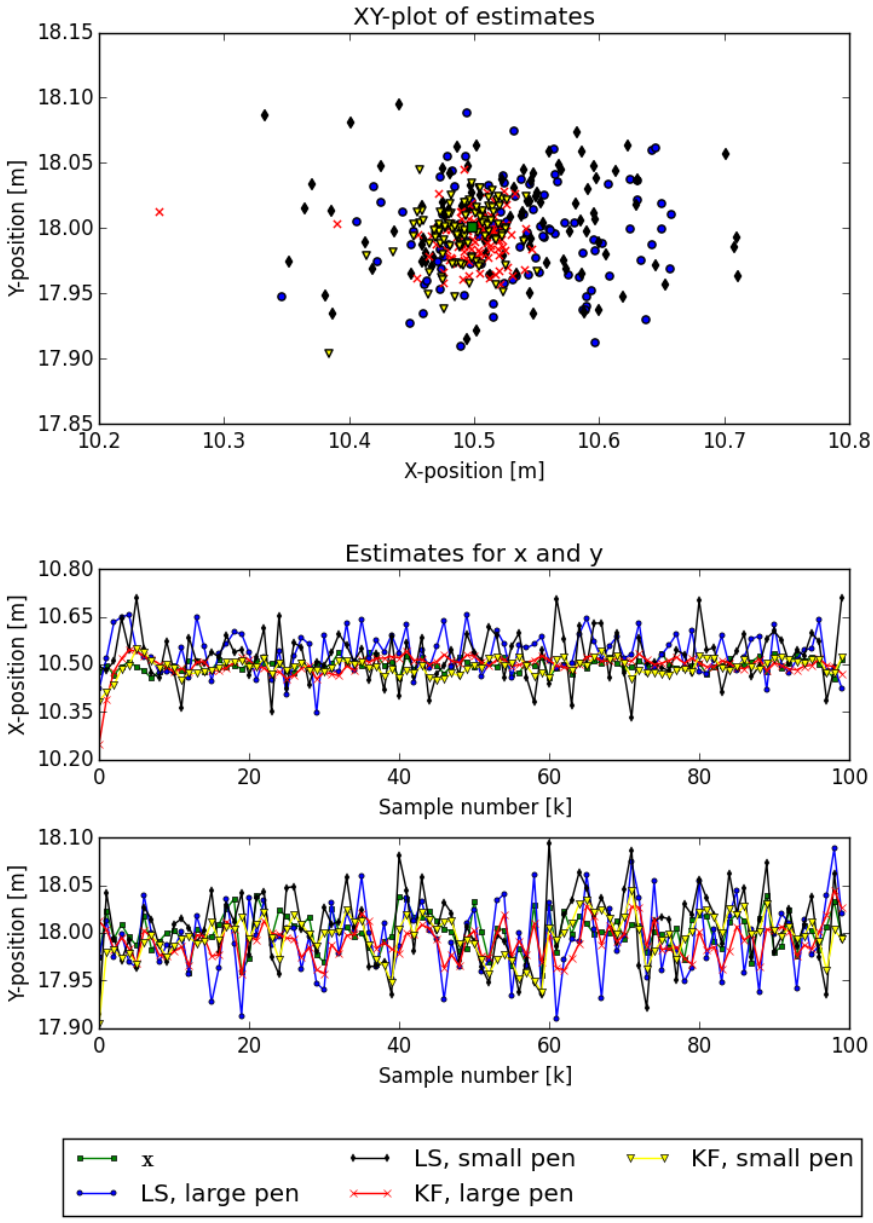

Figure 7.3: The top figure shows the xy plot of the estimates and the bottom figure shows the estimate for each time step. The LSE have a higher variance than the KFs.

7.3 Simulation of case 3

Case 3 was designed to investigate how the disfiguring of the pen would affect the position estimation.

7.3.1 Simulation setup

The same setup was used for case 3 as was used for case 2. A zero mean Gaussian error with a standard deviation of 20 centimeter were added to the remote anchors. The value of 20 centimeter was picked after recommendation from the people at SMS with experience from the field. As the case is set up to examine the affect of anchor displacement, the exact value is not important.

7.3.2 Result

The result of the simulations of case 3 can be found in Table 7.2 and Figure 7.4. The remote anchors were moved 30 and 10 centimeters which resulted in an over 10 centimeter higher CDF value. Because of the displacement of the anchors, a bias is observed in the estimates. Even though the CDF value of the KF is acceptable it is possible for the disfiguring to become larger and measures should be taken to rectify such errors.

	LS (large)	LS (small)	KF (large)	KF (small)
CDF [m]	0.342	0.250	0.176	0.171
RMSE [m]	0.256	0.175	0.142	0.140
STD [m]	0.081	0.080	0.033	0.030
Mean error (x)	0.107	0.092	0.033	0.034
Mean error (y)	-0.219	-0.130	-0.133	-0.132

Table 7.2: The Table shows some statistical values for the simulations of case 3. The estimators have a significantly worse performance than in case 2.

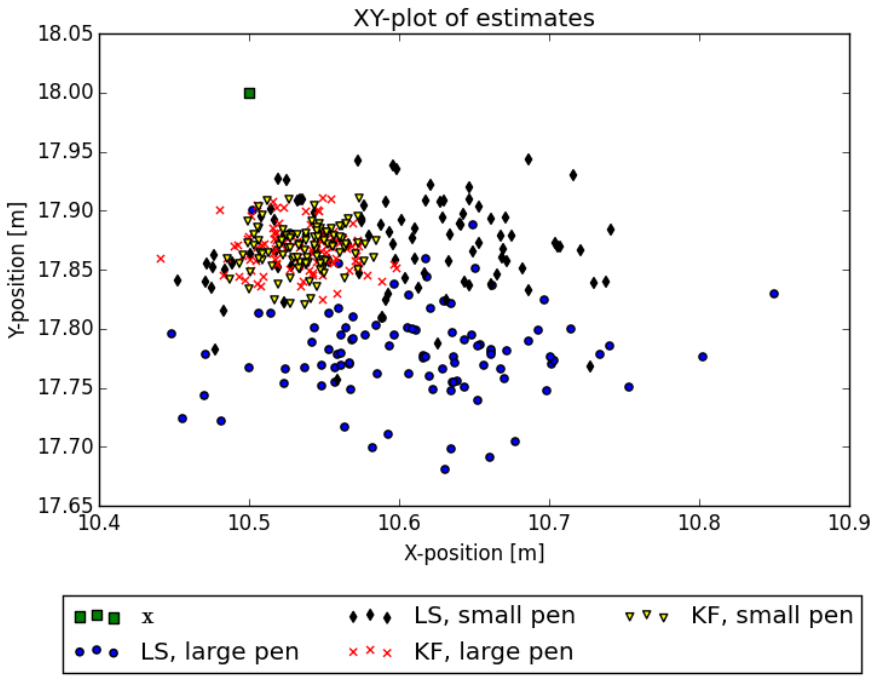

Figure 7.4: The figure shows the xy plot of the estimates in case 3. With a displacement of the anchors, a significant bias is observed.

7.4 Simulation of case 4

The simulations modeled a localization scheme where two remote anchors were positioned with an equal distance from the center anchor. Because it would be convenient when conducting the field tests later, the anchors were chosen to form a straight line. This lead to the center anchor having the position $(0.0, 0.0, 1.2)$ and the remote anchors the position $(\pm L, 0.0, 1.2)$, with L being 2.5 and 7 meters for the short and long cases. The buoy's position was Gaussian distributed with the center at $(0.0, 18.0, 0.0)$ and uncorrelated standard deviation of 2 centimeters in both x and y direction. The measurements were modeled as in Equation 6.3 with a standard deviation of 5 centimeters. The assumption of an error with standard deviation of 5 centimeter is rather pessimistic compared to what DecaWave state in the data sheet of the DW1000 chip[1] where it's given to be approximately 2 centimeters.

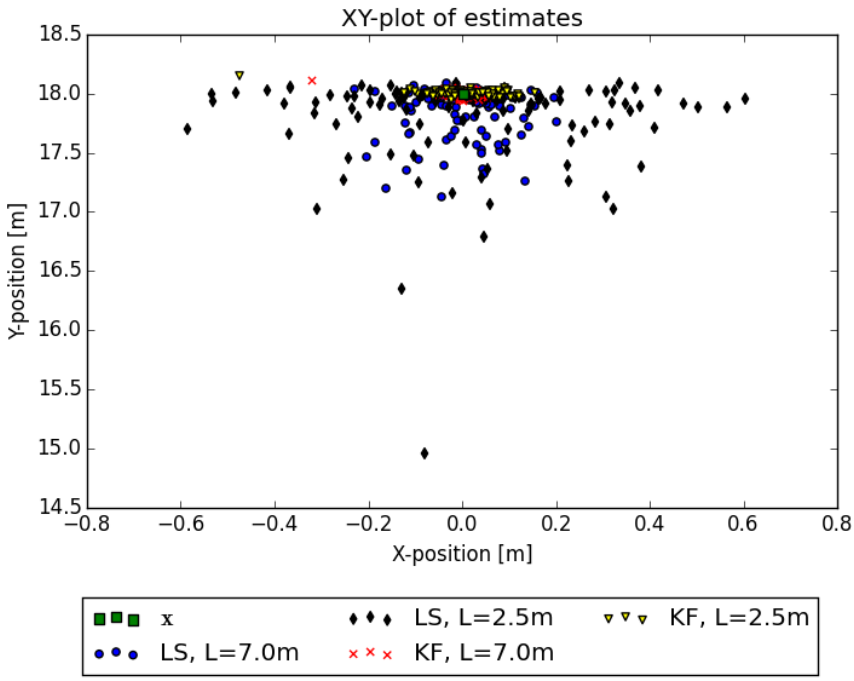

Figure 7.5: The Figure shows the LS and KF estimates of the buoy. As seen from the Figure is the variance of the KF estimate significantly smaller than the LS estimate. The green square is the mean position of the buoy.

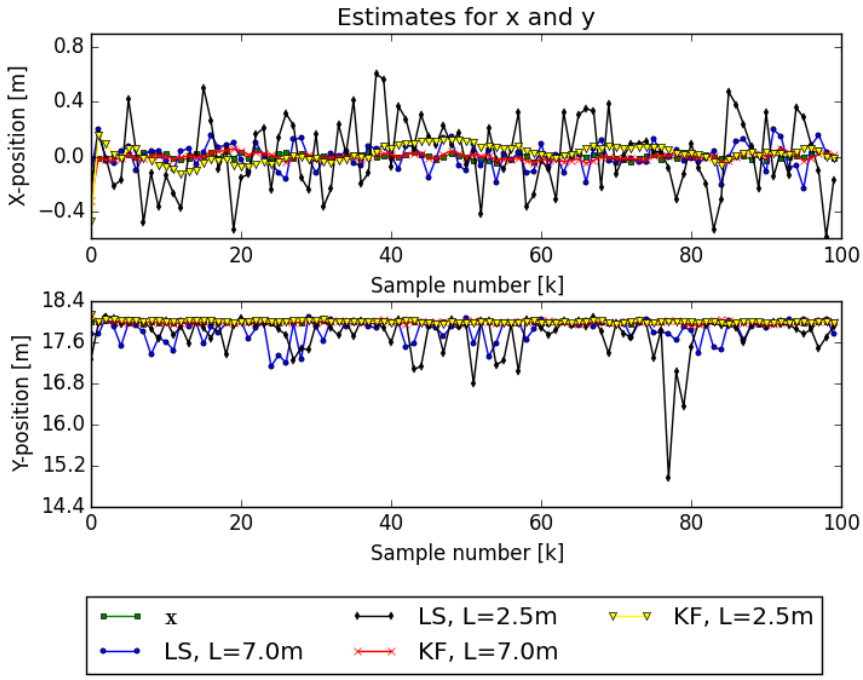

Figure 7.6: The Figure shows how well the LSE and KF estimators follow the true position of the buoy. The LS estimator performs significantly worse than the KF estimator and have a much higher variance.

7.4.1 Results

Figure 7.5 - 7.7 show the results of the simulation. Quantified performance parameters can be seen in Table 7.3. Figure 7.5 shows how the estimates spread out in the x-y plane. As seen from the figure, the KF performed significantly better than the LSE and the difference was even greater than with the previous two cases. The LSEs had a much higher variance and outliers with an error of more than 1 meter. With the KF, no outliers were observed even with the short distance setup.

Figure 7.6 shows how well the estimators performed at each time step for both x and y states. The Figure backs up what could be seen from Figure 7.5 as the LSE had a much higher variance than the KF. The higher variance of the LSE comes from the lack of filtering of the data and is a disadvantage as it means the state estimate is significantly less reliable. Figure 7.7 shows the distance error from the buoy to the state estimates. It shows how superior the KF is compared to the LSE as almost every point is closer to the true position.

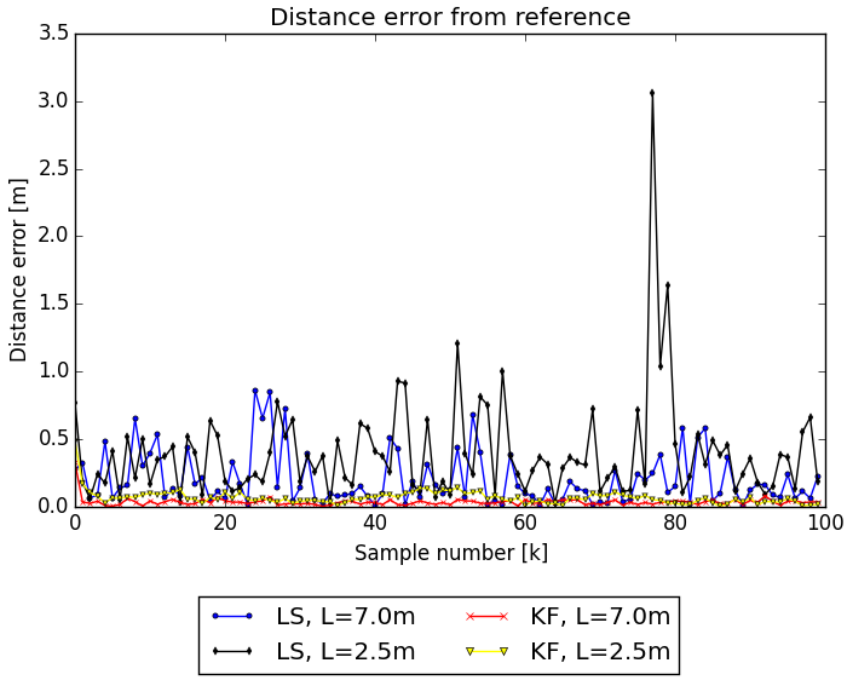

Figure 7.7: The Figure shows the performance of the LS and KF estimators

	LS (long)	LS (short)	KF (long)	KF (short)
CDF [m]	0.679	1.036	0.066	0.134
RMSE [m]	0.282	0.551	0.047	0.084
STD [m]	0.236	0.497	0.046	0.080
Mean error (x)	-0.000	0.011	-0.005	0.012
Mean error (y)	-0.157	-0.237	0.003	0.003

Table 7.3: The Table shows the mean and variance of the errors of the estimators. As seen from the Table are both estimators practically unbiased, but the variance of the KF estimator is smaller which leads to a smaller distance error.

With the LSEs having a CDF value of 67 and 103 centimeters, they are not performing sufficiently well. They have a large variance due to the geometric properties of the system. The DOP value for the short and long setups are 5.9 and 3.6 respectively. This helps explain the higher variance in the short case as errors in the range measurements would cause larger errors in the position estimate.

On the other hand, the KF had a CDF range of 6.6 and 13.4 centimeters which is

considered sufficient. The satisfying performance of the KF, even when the sensors had a distance of less than 3 meters lead to the decision to proceed with the field tests for case 4. The results were promising as they seemed to handle the challenges regarding the small sensor surface very well.

Chapter 8
Field Tests

It was necessary to conduct some field tests to evaluate the performance of the DW1000 sensors. Because creating own test modules for the DW1000 IC would have been time consuming it was decided to use the evaluation kit that DecaWave offer. The sensors' were tested inside a gymnastic hall, at a football field and at docks by the water.

8.1 TREK1000 Evaluation Kit

The TREK1000 Evaluation Kit is a kit offered by DecaWave to evaluate their DW1000 sensors. The kit contains four identical circuit boards (Figure 8.1) with various functionality. They can be set up as either an anchor or a tag by turning the switches on the board. Additionally, a display is mounted on each circuit board to give information on its configuration and measurements.

Application and data extraction

A useful feature of the evaluation kit is the existing software DecaWave offer. They have made an application that is good to go, apart from downloading a driver and connecting one of the circuit boards through a USB cable. The application has a visual interface and the ability to get the tag coordinates. However, the interesting parts are the distance measurements as that is what the sensors will be used for in the real world application. The distance measurements are available through a logging feature where the application writes various data to a text file. The text file can be parsed in a python script and the measurements extracted.

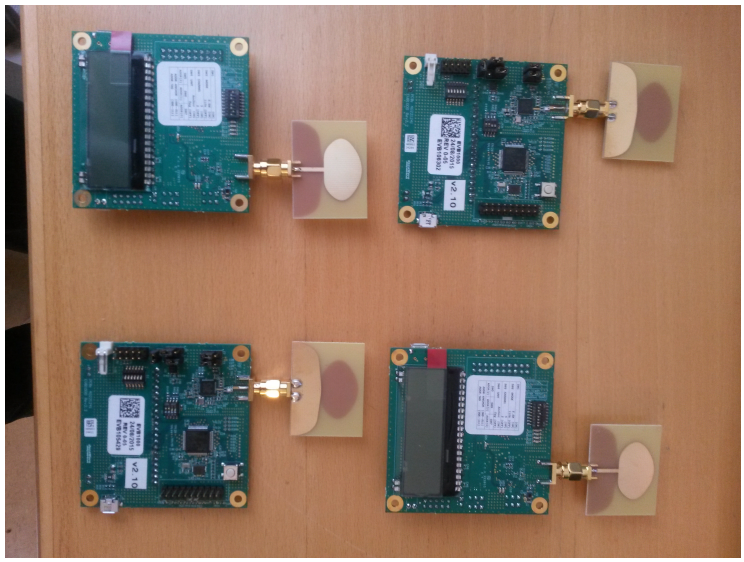

Figure 8.1: Front and back side of the four UWB ranging nodes in the TREK1000 Evaluation kit. Having four ranging nodes gives three anchors and one tag.

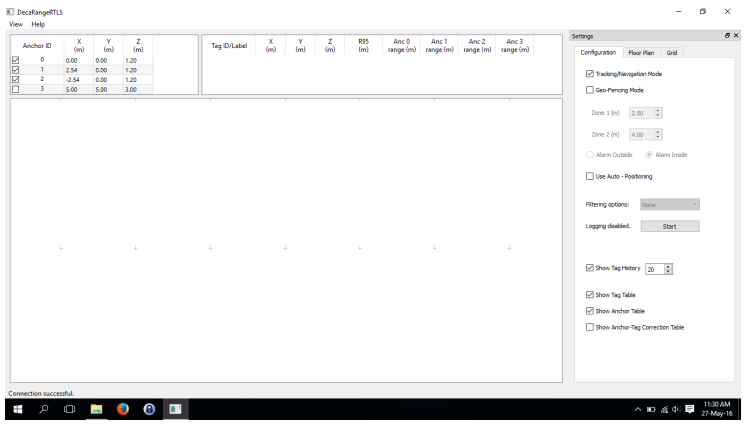

Figure 8.2: The desktop application that DecaWave deliver offers an easy way of getting the evaluation kit up and running. The *Start* button to the right gives the opportunity to log the measurement data.

8.2 Case 1: Validation of sensors' performances

To get an indication of the DW1000's ranging performance, the nodes of the TREK1000 Evaluation Kit had to be tested. DecaWave state in the DW1000 data sheet[1] that the sensors typical error probability distribution is a zero-mean Gaussian with a standard deviation of 2 centimeters. This needed to be validated in order to get an indication of how well the localization algorithm could perform.

8.2.1 Set up

Location

Because of the uncertain weather conditions in Trondheim at the time the experiment were to take place, the measurements had to be done indoors. Norwegian University of Science and Technology's Sports Association (NTNUI) have several indoor sports halls at their disposal that are available for members to borrow. It was necessary to have an entire hall to get a large enough distance between the sensor nodes. An advantage using a sports facility was the lines and markings that are drawn on the floor. These markings made the setup of the system a lot easier.

Placing of equipment

The tests were split into three similar parts, one for each anchor. Two tripods were used, one for the tag and one for the anchor to be tested. The tag was mounted on the tripod and positioned on one end of the hall. The anchor to be tested was connected to a computer and mounted on top of a tripod with fixed position at the other end. To make the distance between the two nodes easier to measure, the height of the two sensors were adjusted to be the same. This gave the opportunity to measure the distance between the nodes along the floor. A tape measure was used to measure the reference distance (Figure 8.3).

8.2.2 Results

Distribution of error

Histograms of the measurements from each anchor can be seen in Figure 8.5. The Figure also show a Gaussian curve fitted to the measurement data and the reference value measured using the tape measure in Figure 8.3. The reference value was measured to be 26.07 meters. More specific values of the measurement data, such as mean and standard deviation, are found in Table 8.1. The histograms show that the normal distribution is a fairly good approximation of the measurements. A good indication of this, besides the shape of the histogram, is that there are very few measurements in the tails of the normal distributions and almost all points are within 3σ (99.7 %).

Figure 8.3: The tape measure used to measure the reference distances in the tests.

Measurement bias

As seen from Figure 8.5 and Table 8.1, all the sensors have a tendency to measure a lower distance than the reference distance. The mean distance values also differs with 2.5 centimeters for the different anchors. As the number of measurements for each anchor is large, the confidence interval for the mean and variance are quite small and only spans a few millimeters. The reference measurement and setup was done manually which introduces the likelihood of human error. A reason for the difference in the measurements for the various anchors could be a slight variation in their position when mounted on the tripod. The plastic stand that was holding the circuit board (Figure 8.4c) had a crack that would only allow the position of the circuit board to be varied in directions perpendicular to the tag. With a distance of 26 meter, moving the anchor 10 centimeter in each orthogonal direction would only increase the measured distance by 0.5 millimeters. The anchors were not displaced by 10 centimeters in either of the orthogonal directions which leads to the conclusion that some bias was introduced by the sensors.

Another significant trend in the tests was the difference between the distance measurements of all the anchors and the reference distance. The reference measurement was done by a tape measure (Figure 8.3). When using said device, there is a chance that the tape is not lying on a straight line or completely stretched out. The sensor nodes were positioned such that one of the straight lines on the floor was reaching from one node to the other. This way the line could be used to indicate that the tape measure was stretched out and lying on a straight line. It is not easy to conclude whether the error comes from the sensors or the reference measurements.

(a) The anchors were mounted on a tripod and connected to a computer to extract the measurements.

(b) Because of the height difference of the two tripods used in this experiment, one of the tripods had to be positioned on top of a table to make their height level.

(c) The tag node was positioned on a tripod at one end of the gym hall and its position stayed constant throughout the experiment.

(d) Example of a power bank that was used as power supply for the circuit boards.

Figure 8.4: Pictures from the sensor validation tests.

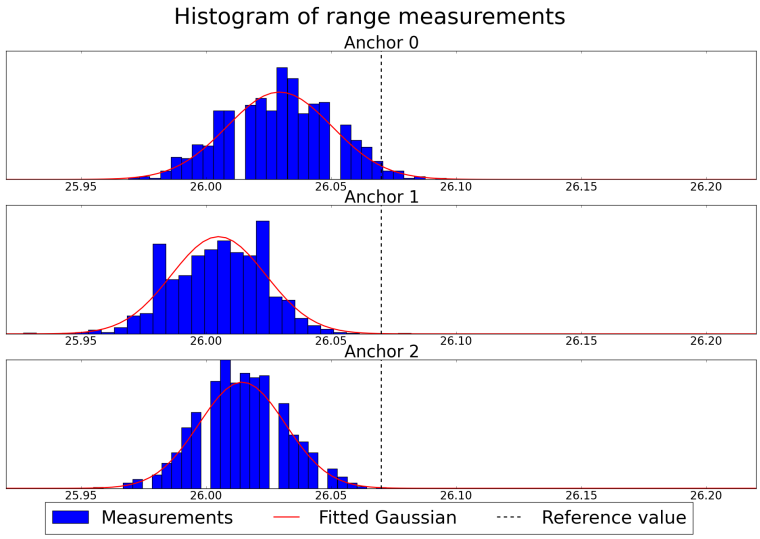

Figure 8.5: Histograms of the measurements for each anchor and their fitted Gaussian curve.

Anchor (#)	Number of samples (N)	Mean (μ) [m]	Standard deviation (σ) [m]	Confidence interval (μ) [m]	Confidence interval (σ) [m]
0	775	26.029	0.021	[26.028, 26.031]	[0.020, 0.022]
1	1078	26.005	0.019	[26.004, 26.006]	[0.018, 0.020]
2	1318	26.014	0.017	[26.013, 26.015]	[0.016, 0.018]

Table 8.1: Statistical data of the range measurements. The confidence intervals assume that the data points are normally distributed and show the 95% confidence interval. Because of the large sample size, the 95% confidence intervals are very small. The intervals assumes normally distributed data.

8.3 Case 2: Localization with sensors surrounding tag

8.3.1 Set up

Location

It was important to to test the sensors over a large enough distance. The largest fish pens in Norway have a cross-section of 50 meter, thus an area that covers at least 50 meters from one side to another was needed. Because of its size and availability, the football field next to the university campus was chosen to be the location where the experiments were carried out. The football field is made of artificial grass and lays in a small pit where there was expected to be an insignificant amount of disturbances from electronic equipment. Besides having a large clear area, the markings and lines on the field made the measuring of the setup significantly easier.

Placing of equipment

The sensors were positioned according to Figure 7.1 and the markings on the field. For convenience, the coordinate frame was also chosen to correspond to the frame in Figure 7.1 with origin in the anchor to the bottom left (anchor 0). The markings on the field did not coincide perfectly with the distances chosen in the simulations, but was not considered a problem as the values had a divergence of less than half a meter. As with the simulations, the anchors forming the baseline had a constant position throughout the experiment. It was only the top anchor's position that was altered. This lead to anchor 0 & 1 having the positions $(0.0, 0.0, 1.2)$ and $(21.0, 0.0, 1.2)$ respectively. The last anchor had two different positions, $(10.5, 33.6, 0.42)$ for the small configuration and $(10.5, 67.2, 0.42)$ for the large one. These configurations correspond to fish pens with radii of 18.44 and 34.42 meters. The tag was positioned on top of an aluminum bucket that could reflect the signal, possibly create MPCs and protect it from unknown materials on the field ground.

8.3.2 Results

Figure 8.7 - 8.9 shows the results of the experimental tests. The CDF value was slightly bigger for the field tests than what was seen in the corresponding simulations. From Figure 8.7 and Table 8.2, it can be seen that this was mostly due to the bias of the estimates. The STD of all measurements were smaller than what was experienced in the simulations, most likely because of the simulations assuming a too large variance in the range measurements.

The simulations of case 3 showed that a wrong assumption of the anchor positions leads to a bias in the state estimates and inaccuracies when setting up the system could have caused the bias observed. The bias in the range measurements detected in

(a) Overview of the setup used in the tests. The markings on the field were used to improve the accuracy of the setup. The setup were measured with a tape measure to get the reference positions of the various components.

(b) Close-up of the workstation where the computer was connected to an anchor to extract the data.

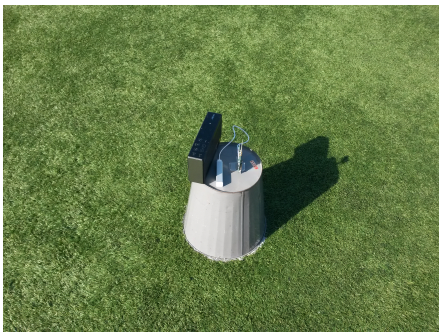

(c) The tag node was placed on top of an aluminum bucket to avoid placing it directly on the field. An attempt to disturb the RF-signals using a speaker communicating with Bluetooth was also carried out, but proved to be unsuccessful.

Figure 8.6: Pictures from field tests for Case 2

section 8.2 could be a source as well. Most likely, the bias is caused by a combination of the two.

Both estimators showed a sufficiently small CDF for both filters to be accepted as solutions. This is advantageous as the model of the BU used in the KFs might prove to be wrong when applied in the real world. As the tag in the experimental tests had a fixed position, the tests suffer from the lack of natural BU movement and gave no indication on whether the model is accurate or not. The LSE performing satisfyingly offers an alternative estimator with no prior knowledge of the BU behavior required.

	LS (large)	LS (small)	KF (large)	KF (small)
CDF [m]	0.137	0.108	0.098	0.082
RMSE [m]	0.083	0.069	0.076	0.066
STD [m]	0.039	0.030	0.015	0.016
Mean error (x)	0.073	0.057	0.072	0.056
Mean error (y)	-0.002	-0.024	-0.020	-0.029

Table 8.2: The Table shows some statistical values for the the experimental tests of case 2. The KFs performs significantly better than the LSEs and both estimators perform better in the small fish pen.

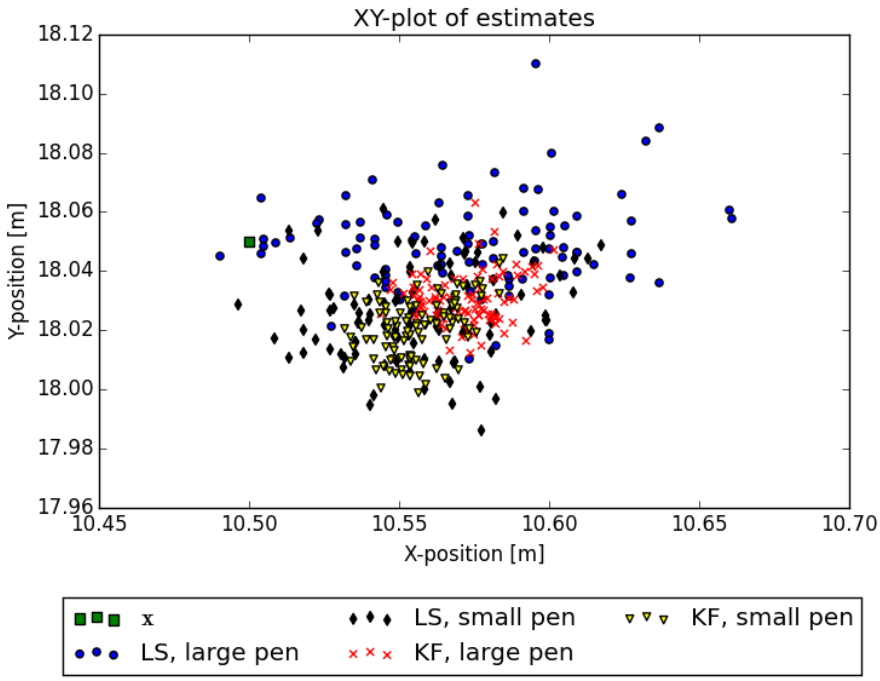

Figure 8.7: XY-plot of the estimations in the experimental tests for case 2. The figure shows a similar behavior of the estimators to what was seen in the simulations, but with a small bias.

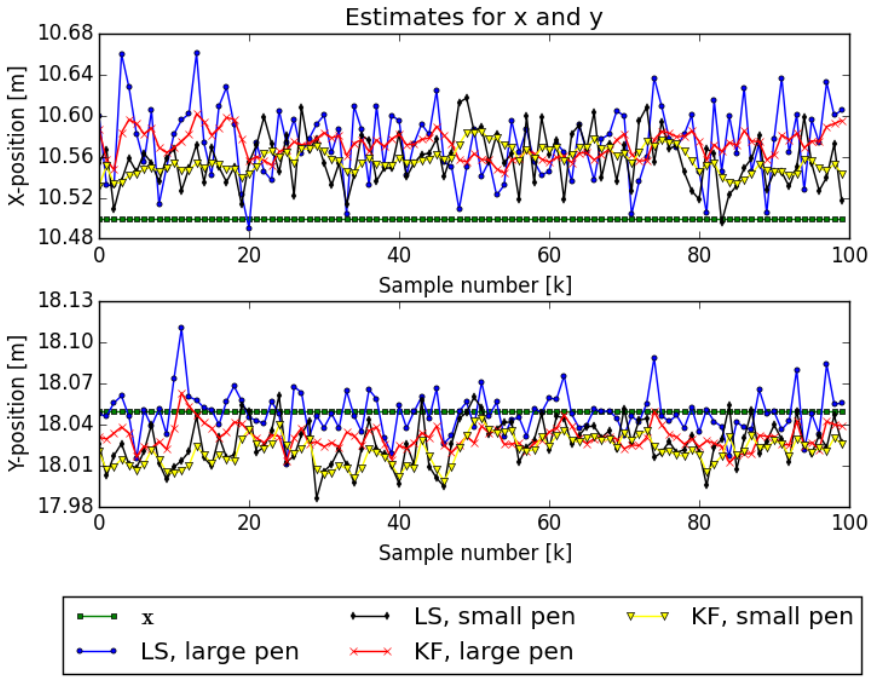

Figure 8.8: X and y estimations for all sample points. The figure shows a bias in the estimate of both states.

Disturbance by other RF equipment

To examine how the sensors would behave in the proximity of other equipment using RF sensors, a speaker communicating with Bluetooth was positioned next to the tag (Figure 8.6c) and a smart phone was connected to the speaker while streaming music. The sensors showed no indications of being disturbed by the speakers. Bluetooth operates in a band with center frequency at 2.4 GHz while the DW1000 sensors operated with a center frequency of 3.5 GHz and their compatibility were expected. There will most likely be no Bluetooth speakers on the fish pen location, but the fish pens are often equipped with WiFi. Several WiFi standards (802.11b/g/n) operates in the same frequency spectrum as Bluetooth and the compatibility with the Bluetooth device indicates this might be the case for WiFi devices as well. The tests also indicates that the DW1000 sensor is not affected by devices operating outside its on frequency band. The center frequency of the DW1000 sensors can be adjusted between 3.5 and 6.5 GHz and gives an option to avoid certain frequency bands if need be.

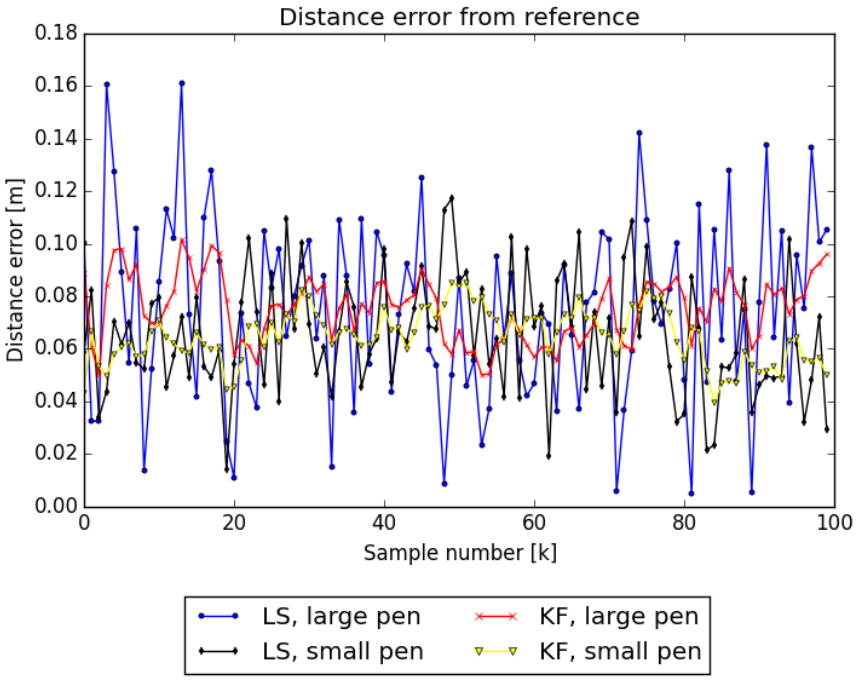

Figure 8.9: Distance error of the estimations.

	Anchor position	
Anchor (#)	Case 4a	Case 4b
0	$(0.00, 0.00, 1.2)$	$(0.00, 0.00, 1.2)$
1	$(2.54, 0.00, 0.79)$	$(7.26, 0.00, 0.79)$
2	$(-2.54, 0.00, 0.79)$	$(-7.26, 0.00, 0.79)$

Table 8.3: Table showing the different placement of the anchor nodes for case 4 and 5.

8.4 Case 4: Localization with close sensors

Because of the reasons discussed in section 3.4, it was important to examine how well the localization system could perform when the anchors were narrowly positioned. The position of the sensors have a great impact on the accuracy of the position estimate, but as seen in section 7.4, the accuracy could be significantly improved by applying a Kalman filter (KF). This needed to be validated in the field tests.

8.4.1 Set up

Location

The tests for case 4 were carried out on the same field as the one used for case 2.

Placing of equipment

The anchors were positioned on flat line because it made the setup of the tests more straightforward. This is because it coincided with the given lines and markings on the field. Two different lengths between the remote anchors and center anchor were tested. A sketch of the setup can be seen in Figure 8.10 and the positions of the different nodes can be seen in Table 8.3. The center anchor had the position $(0.00, 0.00, 1.20)$ and was connected to a computer running the DecaWave application.

8.4.2 Results

Results from the localization tests can be seen in Figure 8.12 - 8.14. As with the simulations, the KFs performed significantly better than the LSEs. The KFs were tuned to assume small variations in the position of the tag, even though it was stationary, to make their behavior more similar to what it would be in the real application.

The results of the tests demonstrates the disadvantages of placing the sensors close to each other. For both setups, the LSE have an unacceptably large CDF value. It was desired to have a 96 % certainty range of maximum 25 centimeters which was

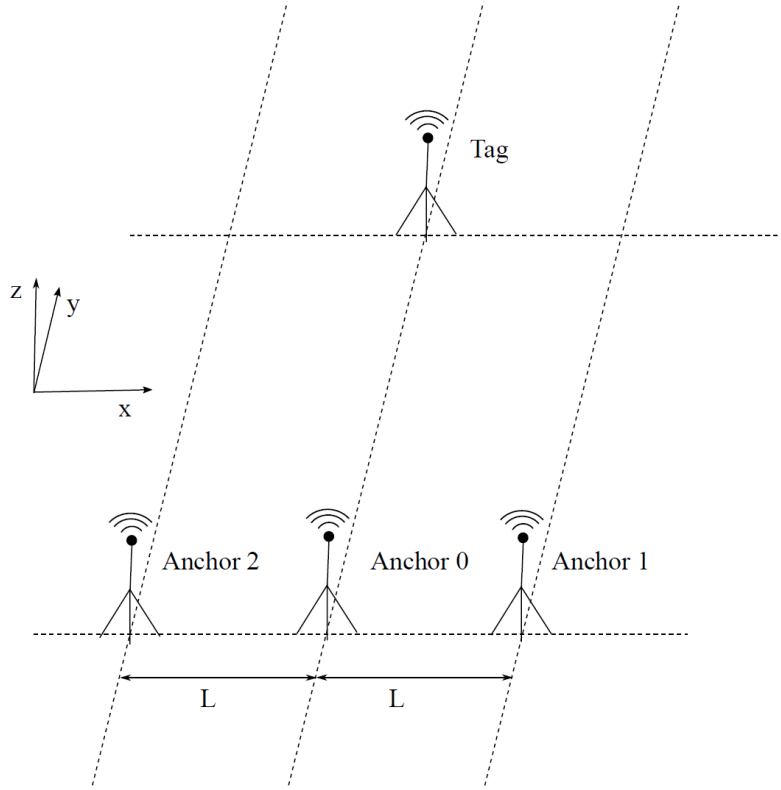

Figure 8.10: The Anchors were positioned on a flat line with a small distance between them. This was to examine how well the sensors are able to localize the tag when positioned close.

only achieved by the KF with the long setup. However, the DOP value changes with the position of the tag and it is likely that if the tag were placed in another position the estimates would be poorer. In section 3.4, Figure 3.7 show that the DOP value becomes larger with a longer distance from the sensors. For the currently tested position of the tag, the DOP value is 3.6. However if the tag were positioned 20 meters further away from the sensors, the value would be almost 5.0. This is likely to make the KF perform worse.

8.4.3 Bias problems

The xy-plot in Figure 8.12 shows the significant bias of the estimates. The KF's estimates is much better in the y-direction, but have the same bias in x-direction.

The bias in x-direction can be explained geometrically. Figure 8.15 show the 3 circles that corresponds to the averaged distance measurement for the 2.54 meter

(a) The field on which the tests were executed.

(b) Example of the closest setup of the anchors. The anchors were placed at a greater distance as well.

(c) The tag node was placed on top of an aluminum bucket to avoid placing it directly on the field.

(d) A human blocked the tag node to see how well the sensors would perform in conditions with no line of sight.

Figure 8.11: Some illustrating pictures from the experiment.

setup (Table 8.5). There is no single point where all circles intersect which leads to the most likely point for the tag (x) to be the point that minimizes the squared distance to each sphere (section 4.1). The mean range measured from anchor 1 (positioned on the right) is 12 centimeter longer than the mean range measured by anchor 2 (positioned on the left). However, these 12 centimeter pushes the estimate 40 centimeters to the left. This shows the geometrical disadvantage of placing the sensors too close.

When the distance between the anchors is increased, the estimate improves significantly in the KF case. The improvement is not as good for the LSE, but it does not have the same amount of bias to the left as when the sensors were closer. Reasons for the lack of drift could be the improved geometric conditions that having a greater distance between the sensors causes, as well as the smaller difference between the average distance measured by the two remote anchors.

	LS (long)	LS (short)	KF (long)	KF (short)
CDF [m]	2.255	1.234	0.168	0.470
RMSE [m]	1.268	0.854	0.157	0.444
STD [m]	0.411	0.291	0.010	0.023
Mean error (x)	0.030	-0.437	0.030	-0.435
Mean error (y)	-1.200	-0.673	-0.154	-0.089

Table 8.4: The table shows the some properties of the estimators. As seen from the table are both estimators practically unbiased, but the variance of the KF estimator is smaller which leads to a smaller distance error.

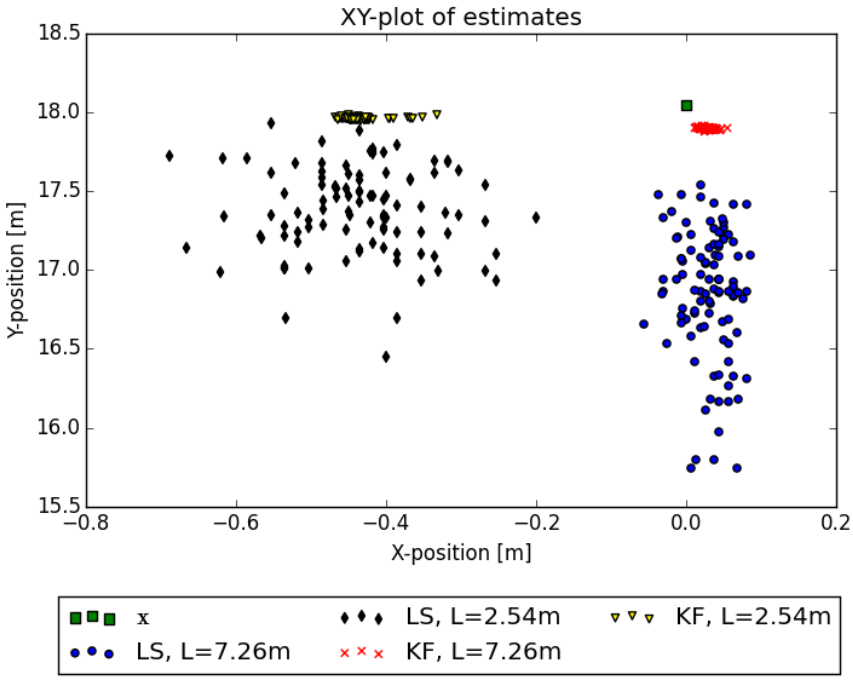

Figure 8.12: XY-plot from the localization tests. When the distance from center anchor to the remote anchors were 2.54 meters, the localization performance was poor for both estimators. Increasing the distance to 7.54 made the KF behave significantly better. Notice that the distribution of the LS estimations changes with different sensor configurations.

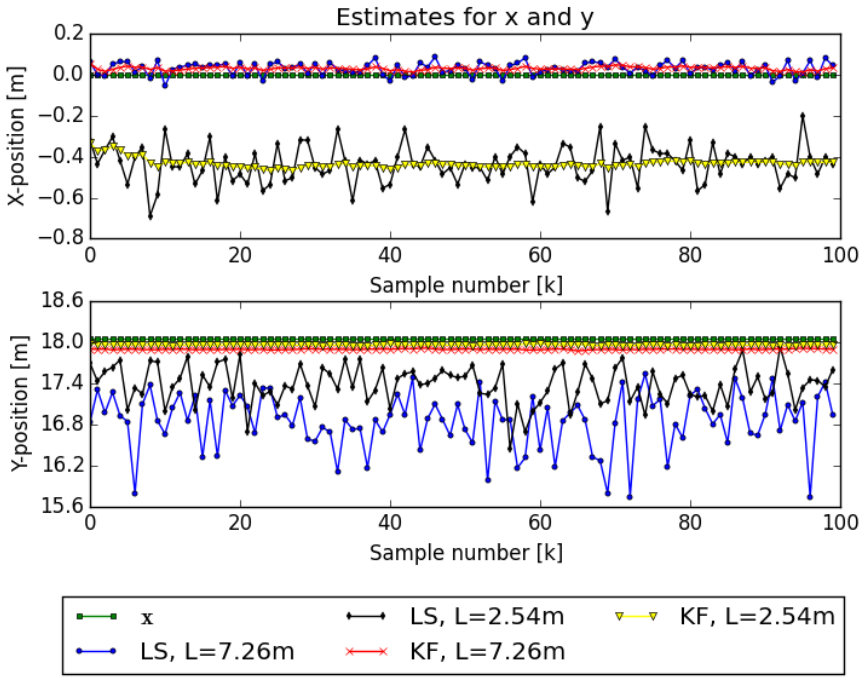

Figure 8.13: The Figure shows the performance for the estimators for the x and y coordinates. It can be seen that all estimators estimated the y-coordinates to low. This might be because of the bias that was discovered in the sensor validation tests 8.2.

	Average measured distance (μ_z)	
Anchor (#)	Case 4	Case 5
0	18.04	17.99
1	18.18	19.26
2	18.06	19.29

Table 8.5: The table shows the average value of the distance measurements from each anchor for both cases.

.

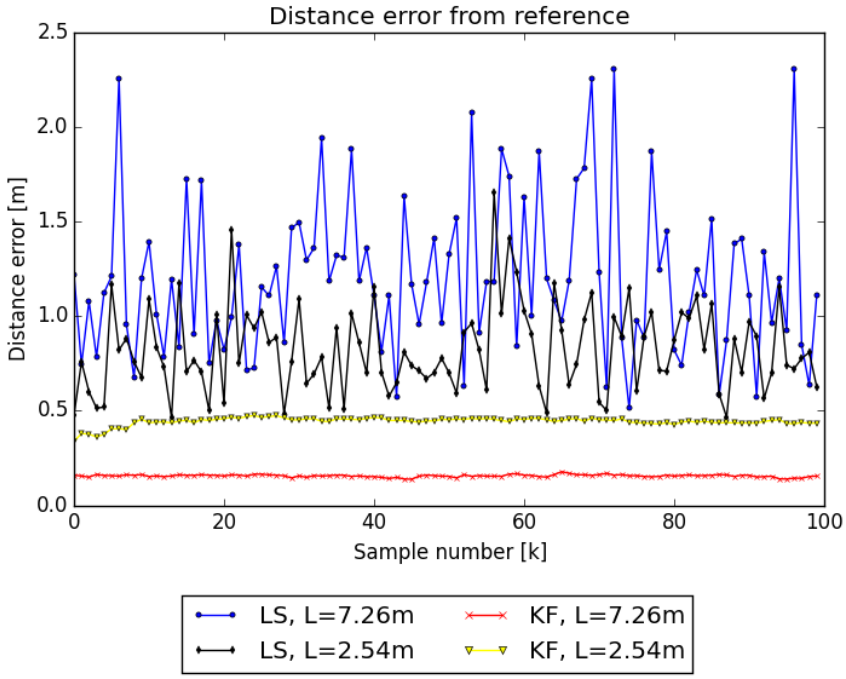

Figure 8.14: The Figure shows the distance error of the different estimators. The KFs perform significantly better than the LSEs. When the distance between the sensors were 7.26, the KF achieve a distance error of approximately 0.17 meters.

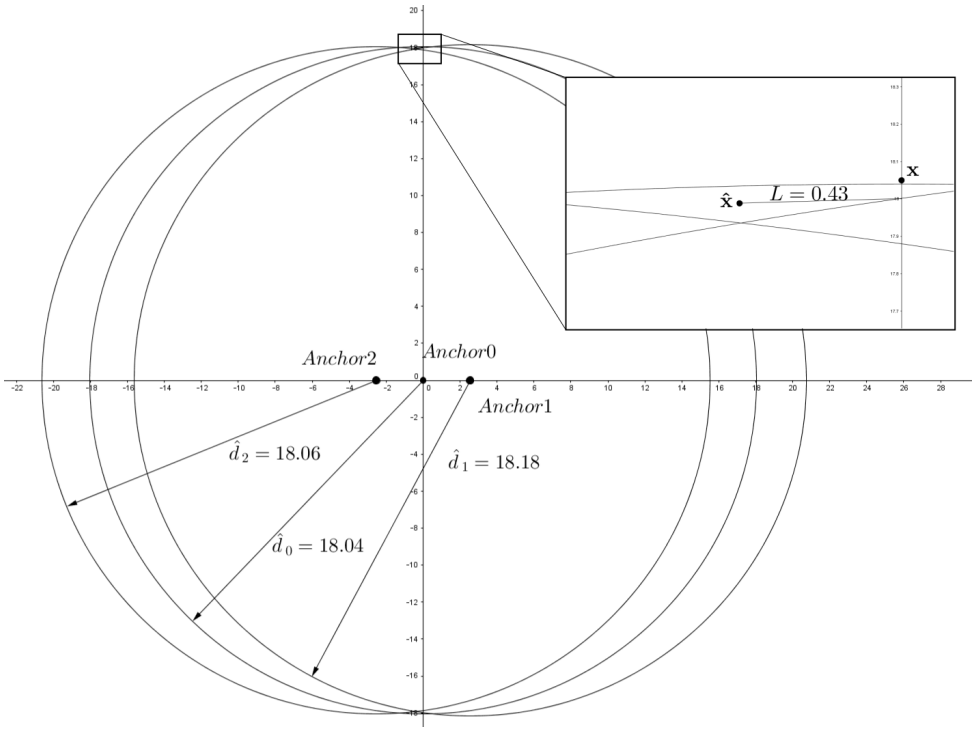

Figure 8.15: The radius of the circles corresponds to the average range measurements from the case 4 tests. $\hat{\mathbf{x}}$ is the solution to the LS problem and the most likely position of $\mathbf{x}$. It is seen from the image that a difference between the circle from anchor 1 and 2 of 12 centimeter 43 centimeter to one side. This clearly illustrates the disadvantages by positioning the sensors too close.

Obstruction of Tag

To examine the sensors' ability to penetrate obstacles, a human block was introduced. How this was done can be seen in Figure 8.11d. The human block caused some problems as it was harder for the sensors to receive a signal. An interesting effect of putting a block in front of the tag was the increased distance measured. When the block was introduced the average distance measured was 14.9 centimeters longer than with a clear line of sight. This could be because the signal did not penetrate the human block, but was rather MPCs reflected of the field and therefore traveled a longer distance.

8.5 Case 5 & 6: Performance of sensors near water and with obstruction

In order to examine the sensors' suitability for integration with the relevant system, the sensors needed to be tested in an environment similar to the one they will experience on location. There are mainly two concerns that arises when considering the sensors' relevant practical abilities, how will they behave in proximity of water and are they able to penetrate the material of the BU? To be able to carry the tests out, some practical challenges, such as making the tag sensor float and still keep it dry, had to be resolved (result can be seen in Figure 8.16).

The format of the log files the DecaWave application produces gave some issues regarding the documentation of the tests. The measurement samples in the log files lacks a time stamp which made it hard to know when the measurements took place, thus making it hard to know how many signals that were missed and how long it took to be able to carry out a measurement. However, within the application, the measurements are updated in real-time which gave an indication of whether there was a connection between the nodes or not. The results of the two tests are based on said real time experience and not data from log files.

Location

The tests were done at a dock facility for private boats. The docks made carrying the tests out simpler as they had a convenient distance between them (approx. 15 meters) and removed the need for a boat. Even though 15 meters is a shorter distance than the diameter of a fish pen it made it possible to go through with the tests given the available equipment.

Setup

Pictures from the setup can be seen in Figure 8.16. The tag was put inside a plastic container. The lid of the container had a bolt through it which enabled a various number of POM plates to be fastened to it. The lid was then sealed using tape. As the plastic container had a lower density than water, and because of all the air it contained, bags filled with sand was fastened to the bottom of the box to give it the right buoyancy (Figure 8.16d). Ropes were also connected to the container to work as a safe line and to help positioning the box (Figure 8.16b). The anchors were placed in a triangle with sides of approximately 16 meters where two anchors were positioned on different docks and the last one on land. The different anchors had different heights over the water.

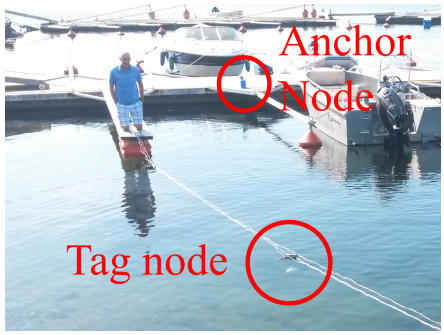

(a) tag node floating in the water surface and an anchor node in the background.

(b) One of the anchors was mounted on a tripod that was positioned on land.

(c) Because of the limited resources available when the tests were carried out, and there was no extra tripod available, one of the anchors was positioned on a pole to give the sensor some height.

(d) The tag was put in a plastic box. Because the box was filled with air, bags with sand were used to get the desired buoyancy.

Figure 8.16: Some illustrating pictures from the experiment.

8.5.1 Test in water with one obstruction plate

With the first test, only one plate of POM was fastened to the floating node. This caused the antenna of the tag to be just above (approx 1 centimeter) the water surface. With this configuration, no noticeable signal loss was observed.

8.5.2 Test in water with four obstruction plates

Three more plates of POM was added to the top of the floating node. The extra weight from the plates made the node lay slightly lower in the water. This caused significant problems with receiving a signal and measurements were only completed sporadically. Lifting the tag a few centimeters, such that the antenna was slightly over water, resulted in the sensor completing measurements at the same rate as was

observed with one layer of POM. This makes it likely that it's the water that was stopping the signals and not the POM plates.

Another noticeable observation was which anchors that were completing the measurements. It was considerably more measurements that were completed for the anchors with a higher position over the water surface. The anchor node positioned at the lowest point (see Figure 8.16a) had significantly more problems with receiving a signal. The high position gave them an angle that would make the signal travel through less water. This builds up under the claim that it was the water that stopped the signal and not the layers of POM.

The results of testing the sensors in water were as expected and gave indications that the sensors could be able to perform well when used near the water surface. There are certain measures that need to be taken to make sure there is an insignificant amount of water between the antenna of the tag node and the anchors. These are discussed further in 9.

Chapter 9
Summarizing Discussion

The following chapter discusses general results and ideas presented in the thesis. Based on the tests and simulations, the chapter reviews the feasible solutions and evaluates their suitability for this particular application. It discusses further work and proposes ideas to deal with expected challenges.

9.1 Suitability of DW1000 sensors

Both ranging ability and robustness of the DW1000 sensors were tested. The distribution of the measurements were similar to a Gaussian distribution with a standard deviation of approximately 2 cm, but with a varying bias of up to 5 centimeters. An explanation for the bias might be some inaccuracies when setting the tests up or bad calibration of the sensors. Antennas are known to cause varying time delays in the measurements due to changes in temperature (stated by DecaWave to be $2mm/C^{\circ}$ for the DW1000 modules[13]). Calibration routines could be added to the system as the anchors will have a fixed position relative to one another given the correct weather conditions. If the relation between the antenna delay and temperature given by DecaWave is sufficient, another option would be to integrate a temperature sensor into the system to correct the bias.

When tested in water, the DW1000 sensor performed satisfactory as long as the antenna was slightly above the water surface. If the antenna were pushed slightly down, the sensors would not receive any signals. This is assumed to be because of the water between the sensors and not the layer of POM as the sensors would have a connection if the tag was lifted slightly. Such behavior sets requirements regarding the antennas position on the BU as it needs to be placed slightly over the water surface. Because of the pulse based ranging technique of the DW1000 sensors, waves covering the BU momentarily should not cause a problem. A small antenna could be placed on an appropriate position on top of the lid. Alternatively, a small room could be cut out of the lid to keep the antenna inside the BU. This would give a

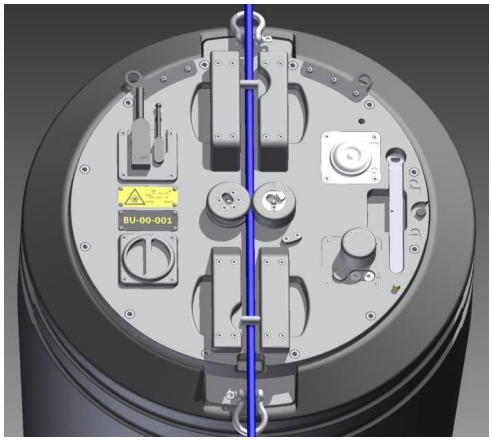

Figure 9.1: The lid of the BU is made of POM and contains various components that need to be taken into consideration when choosing were to put the DW1000 sensors.

smaller amount of material for the radio signals to travel through and slightly elevate the antenna.

9.2 Evaluation of localization performances

The results from the sensor tests are presented in section 8.3 and section 8.4. They showed that when distributing the sensors around the pen, the desired performance was achieved for both state estimators implemented (LSE & KF). The KF performed better than the LSE, but both estimators performing acceptably gives the option of using a LSE in case the model used in the KF does not apply in the real world. With the poor accuracy observed when placing the anchors closely on a line, especially for the LSE, said set up is not considered a suitable option. The KF was able to estimate the position within of 17 centimeters in 96 % of the cases, with a distance of 7.26 meters between the sensors, This was considered acceptable, but was with a stationary tag and would probably perform worse given a tag with less predictable movement. Additionally, placing the anchors on a line made the solution sensitive towards small biases in the measurements.

When the anchors were set up in a triangle surrounding the tag, a 96 % certainty of 10 centimeters were achieved when using the KF. This is considered an accepted performance. With the LSE achieved an accepted performance as well (96 % certainty range of 14 centimeters), setting the anchors up in this way is considered the best option.

As the literature[17] states that adding more nodes give better conditions for the

localization performance, this is an option as well. Because the test kit used in the project only had three anchors this was the number that was used, but could be increased in later parts of the project.

Kalman filter model

If a KF is to be used in the application, some practical issues need to be considered. When using the extended version of the filter, it is important that the initial state is within a certain distance of the true state or the filter may diverge. This could be solved by using the LSE, which requires no prior knowledge of the state, to generate an initial guess.

Another issue is the **Q** matrix of the KF as it describes the uncertainty in the movement of the buoy. This uncertainty will probably change with different weather conditions. An option could be to add an IMU to the BU that provides additional information on the BU's movement, but also work as an indicator of the magnitude of the disturbances from the sea.

9.3 Challenges regarding disfiguring of pen

In subsection 3.1.1, it was introduced how the flexible round pens could cause problems for the localization as the relative position of the anchors could be distorted. This claim was reinforced by the simulations of case 3 (section 7.3. A proposed solution for this was to position the anchors close to each other to make the disfiguring of the pen have less of an impact on their relative positions. Because of the results of the field tests of case 4 showing a lower accuracy than desired, positioning the sensors closely is not considered a suitable option. This means that the possible drift in the anchors' position needs to be measured. A feasible solution to this problem is putting a GNSS receiver on each anchor. Said solution would increase the cost of the localization system substantially, but would be easy to design and implement.

9.4 Limitations of conducted tests

The main limitation is that the field tests were not conducted in the environment the sensors will be used. It was considered appropriate to test the general performance of the sensors before designing modules suitable for testing in a marine environment. As most tests were carried out on land and with a stationary tag, there are no available data to confirm the KF model's feasibility in the real world.

Another disadvantage is the limit of the tests of case 5 and 6. The sensors were only tested within a simple replica of the buoy and may prove to be unsuited for

the task when tested in the real buoy. With fish pens having a larger diameter than what was tested with, problems with receiving the signals might occur as well.

Chapter 10
Conclusion

The DW1000 UWB module tested is considered a suitable sensor option to localize the buoy. Its ability to communicate with the reference nodes when near water was considered satisfying as long as the antenna was slightly above the water surface. A solution using at least 4 ranging nodes is suggested. One node is placed inside the buoy and the remaining three are positioned around the fish pen.

Both simulations and field tests showed that the ranging ability of the sensor was sufficient to provide a desired accuracy when localizing the object, given the reference nodes were positioned in a suitable way. The poor localization results of the field tests, when the reference nodes were positioned close to each other on a line, made said setup an unfeasible option. On the contrary, when the sensors were positioned in a manner such that they surrounded the tag node, a desired localization performance was delivered. To cope with the possible disfiguring of certain pen types, it is suggested to use a GNSS receiver (e.g the Piksi GPS mentioned in section 2.5) to correct two of the reference nodes' position.

When using a Kalman filter to estimate the position of the data, the system had a distance error below 10 centimeters in 96 % of the samples. Whether the model of the buoy movement used by the Kalman filter applies in the real world is not concluded on as the localization tests were carried out on land with a stationary tag node. An alternative is to use a Least square estimator which had a slightly worse performance, but requires no prior information about the buoy movement.

With the tests so far indicating that the DW1000 chip is suitable to be used in the localization system, it is advised to proceed with testing in the real environment. To do this, the DW1000 chip should be integrated with a MC and antenna to create ranging sensors appropriate for use in a fish pen.

References

[1] DW1000 datasheet - dw1000-datasheet-v2.09.pdf. URL http://www.decawave.com/sites/default/files/resources/dw1000-datasheet-v2.09.pdf.

[2] Ewos - benchmark 2016. URL http://akvarena.no/uploads/Foredrag/Fagsamling2016/EWOS.pdf.

[3] Marine harvest - capital markets day 2016, . URL http://hugin.info/209/R/2017365/748522.pdf.

[4] matplotlib: python plotting — matplotlib 1.5.1 documentation, . URL http://matplotlib.org/.

[5] NumPy — numpy. URL http://www.numpy.org/.

[6] Piksi, high precision GPS, GNSS, centimeter-level relative positioning, RTK, dual UART, USB, SBAS signals, correlation accelerator | SwiftNav. URL https://www.swiftnav.com/piksi.html.

[7] rtls | OpenRTLS. URL https://openrtls.com/page/rtls.

[8] Scensor product brief - dw1000-product-brief.pdf, . URL http://www.decawave.com/sites/default/files/product-pdf/dw1000-product-brief.pdf.

[9] SciPy.org — SciPy.org, . URL https://scipy.org/.

[10] Zafer Şahinoğlu, Sinan Gezici, and Ismail Güvenç. *Ultra-wideband positioning systems: theoretical limits, ranging algorithms, and protocols*. Cambridge University Press. ISBN 978-0-521-87309-3.

[11] Robert Grover Brown and Patrick Y. C. Hwang. *Introduction to Random Signals and Applied Kalman Filtering with Matlab Exercises*. Wiley, 4 edition edition. ISBN 978-0-470-60969-9.

[12] Andrew J. Davison, Ian D. Reid, Nicholas D. Molton, and Olivier Stasse. MonoSLAM: Realtime single camera SLAM. pages 1052–1067.

[13] DecaWave. *aps014-antennadelaycalibrationofdw1000-basedproductsandsystemsv1.01-2*.

[14] Dhanya Devarajan and Zhaolin Cheng. *Calibrating Distributed Camera Networks.*

[15] Warren S. Flenniken, John H. Wall, and David M. Bevly. Characterization of various IMU error sources and the effect on navigation performance. URL https://www.researchgate.net/publication/267822063_Characterization_of_Various_IMU_Error_Sources_and_the_Effect_on_Navigation_Performance.

[16] David Eugen Grimm. *GNSS Orientation for kinematic applications.*

[17] N. Levanon. Lowest GDOP in 2-d scenarios. 147(3):149–155. ISSN 1350-2395. doi: 10.1049/ip-rsn:20000322.

[18] Agostino Martinelli. Vision and IMU data fusion: Closed-form solutions for attitude. pages 44–60.

[19] Pratap Misra and Per Enge. *Global Positioning System: Signals, Measurements, and Performance.* Ganga-Jamuna Press, revised second edition edition edition. ISBN 978-0-9709544-2-8.

[20] Stefania Monica and Gianluigi Ferrari. *A Swarm Intelligence Approach to 3D Distance-based Indoor UWB Localization.*

[21] Roland Siegwart and Illah Reza Nourbakhsh. *Introduction to autonomous mobile robots.* MIT Press. ISBN 978-0-262-25699-5 978-0-262-19502-7 978-1-4175-6181-0. URL http://site.ebrary.com/id/10225252.

[22] Stingray Marine Solutions. *video-of-buoy.mp4.*

[23] Qilong Zhang. Extrinsic calibration of a camera and laser range finder. In *In IEEE International Conference on Intelligent Robots and Systems (IROS*, page 2004.

Appendix A
Digital appendix content

The following files and folders are included in the digital appendix.

- sourcecode/
- DW1000 data sheet
- DW1000 product brief
- DW100 antenna delay calibration
- Video of buoy

Appendix B
Test

The source code can be found in the digital appendix. It is divided into three categories, functions, classes and scripts. The functions and classes are tools to execute the scripts.